April 2012

Computational Fluid Dynamics Analysis of Two-Phase Flow in a Packed Bed Reactor

Courtney Lynne Sparrell
Worcester Polytechnic Institute

Hannah Mitsue Duscha
Worcester Polytechnic Institute

Mary Patricia Hesler
Worcester Polytechnic Institute

Computational Fluid Dynamics Analysis of Two-Phase Flow in a Packed Bed Reactor

A Major Qualifying Project Report

Submitted to the Faculty of the
WORCESTER POLYTECHNIC INSTITUTE

in partial fulfillment of the requirements for the
Degree of Bachelor of Science
in Chemical Engineering

Hannah Duscha _____
Mary Hesler _____
Courtney Sparrell _____

April 26, 2012

Approved:

_____

Anthony G. Dixon

Abstract

Multiphase catalytic reactions are prominent in chemical engineering; however it is difficult to achieve efficient reactions. Computational fluid dynamics (CFD) software simulates fluid flow so interactions between phases may be analyzed and improved. This project included use of CFD to simulate an experiment on multiphase flow to compare results on flow regime and pressure drop. Results include discussion of the program's capabilities for conducting this analysis and comparison of simulated flow parameters against experimentally determined values.

Acknowledgements

We would like to extend our gratitude first and foremost to our project advisor, Professor Anthony G. Dixon. His extensive knowledge on our project topic and guidance was invaluable to us throughout the course of our project work.

We would also like to express our many thanks to Siamak Najafi and Adriana Hera for going out of their way to secure resources necessary to our project.

Finally, we would like to thank Jack Ferraro for creating a to-scale model of our project geometry for us to use in the laboratory which helped us to enhance our knowledge of our project geometry setup.

Table of Contents

List of Figures

List of Tables

Executive Summary

A topic of great interest in the chemical engineering field is that of catalytic reactions involving interactions between multiple phases. These reactions often involve the interaction of the gas, liquid, and solid phases, most commonly within a trickle-bed reactor. The most challenging aspect of working with these catalytic reactions is figuring out how to achieve the maximum contact between phases in order to get the most efficient reactions. The study of multiphase flow is therefore important in order to understand how to increase the contact between multiple fluid phases as well as between the fluids and solids. Research on this topic may also lead to knowledge on how to improve other process parameters and keep process costs at a minimum.

One research team headed by Andreas Vonortas in 2010 focused on improving the contact between the gas, liquid, and solid phases in an experiment that was documented as "Fluid Flow Characteristics of String Reactors Packed with Spherical Particles". In this experiment, Vonortas et al. (2010) designed a structured catalyst bed in order to achieve maximum particle wetting so that most of the experiment focus could be directed to the flow phenomena generated by the passing of nitrogen and liquid water through the packed channel. A square duct packed with spherical particles was of particular interest for this project report; the model exhibited flow of nitrogen and liquid water at very low Reynolds numbers within the channel.

The challenge presented by this project was to choose a computational fluid dynamics (CFD) program with which to simulate the experimental setup of Vonortas et al. (2010) and then compare the simulated results against the experimental results. This comparison would determine the effectiveness of a computer-based research method for producing results similar to reality so that in the future reaction efficiency could be tested and improved using CFD instead of a laboratory experiment. The first project goal was to examine the effectiveness of the chosen CFD program, ANSYS 13.0, for producing reliable, accurate two-phase flow simulation results. The second project goal was to complete a two-phase flow simulation and compare the results for flow regime, pressure drop, liquid holdup, and axial dispersion to the experimental results of Vonortas et al. (2010).

ANSYS 13.0 was the primary CFD program chosen for this project, however due to the availability of resources for the project and the variance in capabilities of different CFD programs, FLUENT 6.3.26 (another CFD program) was used in combination with ANSYS to complete the project. By the end of the project, only results pertaining to flow regime and pressure drop were obtained because the flow type and geometry proved difficult to work with. Due to the nature of the multiphase flow, the solvers in ANSYS and FLUENT that were originally selected for the problem were not adequate to calculate realistic data that was representative of the flow. An alternative solver in ANSYS and FLUENT was identified as being promising for obtaining the final results for liquid holdup and axial dispersion, however due to the time constraints of the project this alternative solver could not be fully explored. Recommendations for future endeavors were made based on the results that were obtained, however a major conclusion was that an alternative solver may have been better for researching multiphase flow at low rates in such a unique geometry.

Chapter 1: Introduction

Chemical reactions involving components in multiple phases such as hydro-desulfurization, hydrogenation, and oxidation constitute a large portion of the chemical, petrochemical, and petroleum refining industries. Within these industries, multiphase reaction systems encompass a range of unit operations including riser reactors, bubble column reactors, fluidized bed reactors, packed bed reactors, scrubbers, and dryers (Bakker, Computational Fluid Dynamics Lectures: Lecture 14. Multiphase flow, 2008). The breadth of multiphase reaction systems is expansive, and these systems are therefore a topic of great interest in chemical engineering research. Experiments with multiphase reaction systems have the potential to enhance knowledge about increasing the efficiency of the reaction process, increasing the safety for process operators, and decreasing the overall system cost. The promise of these improvements is what continues to drive experimentation involving multiphase reaction systems.

A multiphase reaction system of particular interest is one involving a gas, liquid, and solid phase; this can be found most commonly in trickle-bed reactors where a gas and liquid phase are passed over solid catalyst particles. Trickle-bed reactors are prominent in industries such as chemical and biochemical plants, wastewater treatment, and agricultural manufacturing (Lopes & Quinta-Ferreira, 2009). Within these industries, trickle-bed reactors are most applicable to hydrocracking, hydro-desulfurization, hydro-denitrogenation of gas oil, catalytic dewaxing of gas and lube oils, and oxidation and hydrogenation of organic compounds. Trickle-bed reactors have been shown to exhibit the most flexibility and simplicity of operation as well as low pressure drop and high reaction efficiency which is why research is continuously conducted in this specific area of reaction engineering (Gunjal et al., 2005).

The challenges associated with efficient, safe, and cost-effective gas-liquid-solid catalytic reactions were recently examined in an experiment conducted in 2010 by Andreas Vonortas and his colleagues Ana Hipolito, Mattieu Rolland, Christophe Boyer, and Nikos Papayannakos. Their results were documented in an article titled “Fluid Flow Characteristics of String Reactors Packed with Spherical Particles”.

Vonortas et al. (2010) argued that typical bench-scale experimental catalytic reactors exhibited irregular packing patterns which led to the incomplete wetting of catalyst particles by the phases being reacted, and therefore led to decreased efficiency during testing. The researchers’ experiment sought to increase the efficiency of catalyst testing by creating a “string of particles” inside the reactor such that maximum contact would be achieved. Vonortas et al. (2010) also experimented with a smaller reactor at a fraction of the size of industrial reactor standards in order to address concerns of cost and safety. The experiment by Vonortas et al. (2010) consisted of three models to demonstrate these criteria; an image of the final experimental setup can be seen in Figure 1 below:

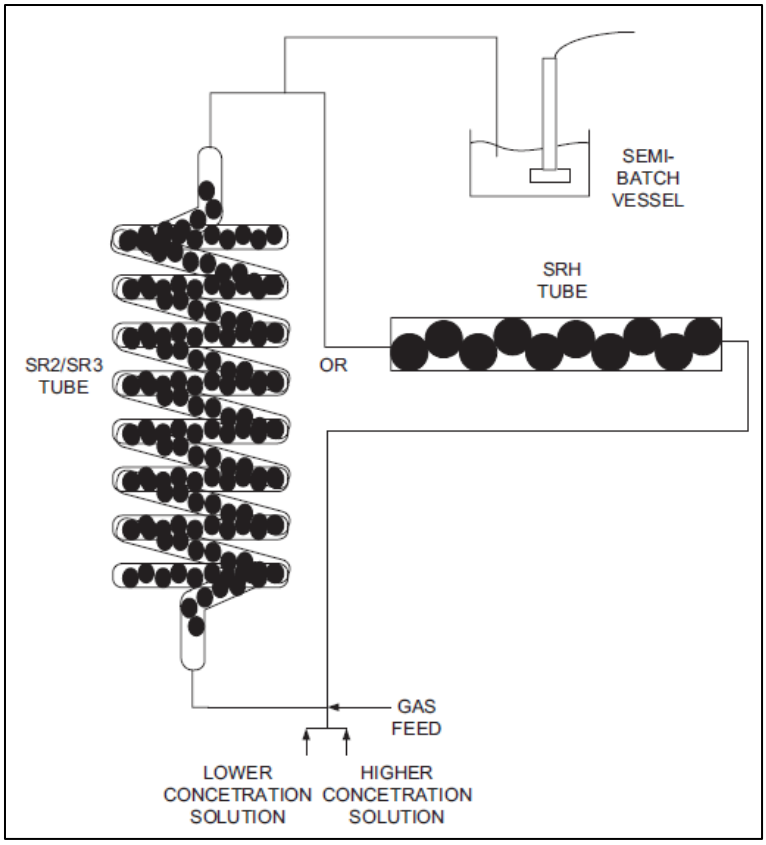

Figure 1: Final Experimental Setup by Vonortas et al. (2010)

The project that will be discussed in this report focused on only the SRH channel as being pertinent to the scope of the project work due to the additional complexity of the geometry of the SR2 and SR3 channels.

Vonortas et al. (2010) specified a model called the horizontal string reactor (SRH channel from Figure 1 above) which consisted of a square channel made of poly(methyl methacrylate) (also known as PMMA) that was laid horizontally and packed with spherical particles. The channel dimensions specified were a cross-sectional area of 16 mm^2 and a length of one meter. The spheres used for packing were made of glass with a specified diameter of 2.9 mm. The multiphase reaction system used liquid water and gaseous nitrogen in co-current flow as the experimental fluids. The assumption of plug flow in both the gas and liquid phase was made in order to simplify the correlations required to examine the flow regime, liquid holdup, pressure drop, and axial dispersion observed in the experiment (Vonortas et al., 2010).

While experiments have been useful for physically observing and examining multiphase reaction system phenomena, they are not necessarily the most time- or cost-efficient means to an end. Computational fluid dynamics, or CFD, computer programs have been suggested as an alternative to physical experimentation which can eliminate the costs associated with obtaining materials to build an experimental model and requiring hours of man labor to conduct an experiment. Given the proper CFD multiphase code, and bearing in mind the limitations of the CFD program's solving capabilities, it may be

possible to reproduce physical experimental results within a small range of error (~5%). CFD can also be useful to test conditions that are not practical to experiment with in the laboratory.

The purpose of this project was to choose a computational fluid dynamics (CFD) program that would be utilized to simulate the experimental horizontal string reactor set-up of Vonortas et al. (2010) and produce results on flow regime, liquid holdup, pressure drop, and axial dispersion for the liquid water-gaseous nitrogen multiphase system. These results were then to be compared against the results of Vonortas et al. (2010) to assess the accuracy of the CFD simulation.

The first goal of this project was to examine the effectiveness of the chosen CFD program, ANSYS 13.0, in producing reliable results that accurately demonstrate physical phenomena in multiphase flow. The second and larger goal of this project was to complete a two-phase Eulerian model flow dispersion simulation for the horizontal string reactor described by Vonortas et al. (2010) in order to compare the results obtained from the CFD simulation to the experimental results reported. Parameters of interest included the flow regime of water and nitrogen in the channel, the pressure drop across the system, the liquid holdup present in the channel, and the axial dispersion observed within the channel.

Chapter 2: Background

Before delving into the specifics of this project, it is necessary to provide the basics of multiphase fluid flow and computational fluid dynamics programs so that the methods and results obtained from this project will be fully comprehensible.

2.1 Multiphase Flow

Multiphase flow played a fundamental role for the duration of this project since the concepts involved in this topic dictated many of the preliminary calculations and assumptions made from which to base experimentation and results. The following two sections elaborate more on multiphase flow basics and practical real-world applications.

2.1.1 What is Multiphase Flow?

Multiphase flow occurs when more than one material is present in a flow field and the materials are present in different physical states of matter or are present in the same physical state of matter but with distinct chemical properties. The materials present in multiphase flow are often identified as belonging to the primary or secondary phases. The primary phase is characterized as the phase that is continuous about, or enveloping of, the secondary phase. The secondary phase is thought to be the material that is distributed throughout the primary phase. Each phase present in multiphase flow may be either laminar or turbulent, which leads to a variety of potential flow regimes for multiple phases in the same channel (Bakker, Computational Fluid Dynamics Lectures: Lecture 14. Multiphase flow, 2008). Some common flow regimes can be seen in Figure 2 below:

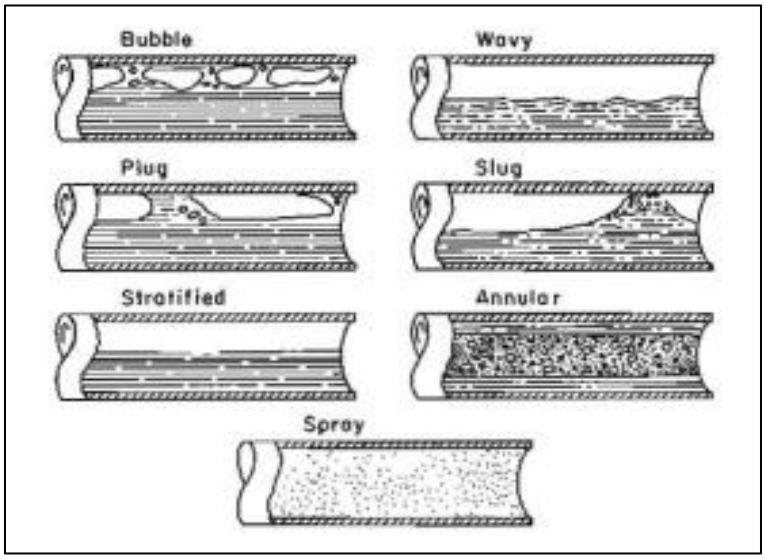

Figure 2: Flow Patterns for Various Multiphase Flow Regimes (Denn & Russell, 1980)

Each flow regime pictured above consists of specific combinations of primary and secondary phases. The description of each flow regime with respect to its primary and secondary phase is summarized in Table 1: Summary of Multiphase Flow RegimesTable 1 below:

Flow Regime Type	Primary Phase/Secondary Phase
Bubble/Plug flow	Liquid/discrete bubbles of gas
Droplet/Dispersed/Spray flow	Gas/droplets of fluid (liquid or gas)
Particle-laden flow	Fluid (liquid or gas)/discrete particles of solid
Slug flow	Liquid/large bubbles of gas
Annular flow	Liquid along walls with gaseous flow core
Stratified/Wavy and free-surface flow	Immiscible fluids; less dense fluid flows atop dense fluid with definitive interface between fluids

Table 1: Summary of Multiphase Flow Regimes (Bakker, Computational Fluid Dynamics Lectures: Lecture 14. Multiphase flow, 2008) (Denn & Russell, 1980)

Multiphase flow can be analyzed further than its flow regime alone by examining the pressure drop across a multiphase system, the liquid holdup observed for the system, and the axial dispersion observed for the system when obstructions are introduced to the channel of flow (such as packing in a catalytic reactor) .

The simplest model that can accurately predict multiphase pressure drop in an empty channel is the Lockhart-Martinelli correlation for binary multiphase pressure drop (Denn & Russell, 1980). In this method, the pressure drop is first determined for both phases as if each phase were alone in the flow field. The method then uses the individual pressure drops for each phase to calculate the Lockhart-Martinelli parameter. This parameter is implemented in the final part of the method in which the Crisholm correlation uses the Lockhart-Martinelli parameter to calculate pressure drop correction factors. These correction factors can be applied to the individual pressure drops for each phase to obtain the total multiphase pressure drop (Calculating Two-Phase Pressure Drop with the Lockhart-Martinelli Method, 2011). Once multiphase flow is applied to obstructed channels, however, methods like Lockhart-Martinelli become inaccurate and experimental methods become necessary to analyze the pressure drop in these systems.

Liquid holdup describes the amount of space that each phase is occupying within the channel of flow and is applicable to packed channels. This is helpful to further describe the type of flow present in a multiphase system, but more importantly holdup provides insight to interphase interactions over a certain period of time, which is useful to know when performing reactor design calculations. Liquid holdup is quantified as the amount of liquid in the channel (usually characterized as height of liquid in stratified flow) divided by the total amount of fluid in the channel (or the total height of the combined fluid flow) (Denn & Russell, 1980).

Axial dispersion describes the extent to which liquid is forced to deviate from its flow path when confronted with an obstruction. This parameter is also applicable only to packed channels. Axial dispersion is correlated with the Peclet (Pe) number, which is a dimensionless measure of how much axial dispersion the flow is experiencing. The Peclet number is most practically implemented as a measure of performance in a reactor and low Peclet numbers are indicative of axial dispersion being counter-productive to reactor performance (Vonortas et al., 2010).

2.1.2 Applications of Multiphase Flow

Multiphase flow is present throughout unit operations in the chemical engineering field, which is why obtaining a thorough understanding of multiphase flow is so important to experimental research and has such broad applications. A summary of important industrial applications for multiphase flow is presented in Table 2 below:

Multiphase Flow Type	Industrial Application
Particle-laden flow (solid in gas)	Pneumatic conveying, fluidized beds, solid separation (filters, cyclones)
Particle-laden flow (solid in liquid)	Stirred vessels, liquid-solid separation, hydraulic conveying
Droplet/Dispersed/Spray flow (liquid in gas)	Spray drying, spray cooling, spray painting
Droplet/Dispersed/Spray flow (liquid in liquid)	Mixing, separations, extraction
Bubble/Plug flow	Flotation, aeration, bubble columns

Table 2: Common Industrial Applications of Multiphase Flow, Adapted from CFD for Chemical Engineers (Andersson, et al., 2012)

As Table 2 indicates, multiphase flow is applicable in a variety of operations including reaction processes, separations, and purification processes. For this particular project, bubble/plug flow was most applicable to the trickle-bed reactors examined by Vonortas et al. (2010). A schematic showing the typical setup of gas and liquid flow across a bed of solid particles in a trickle-bed reactor can be seen in Figure 3 below:

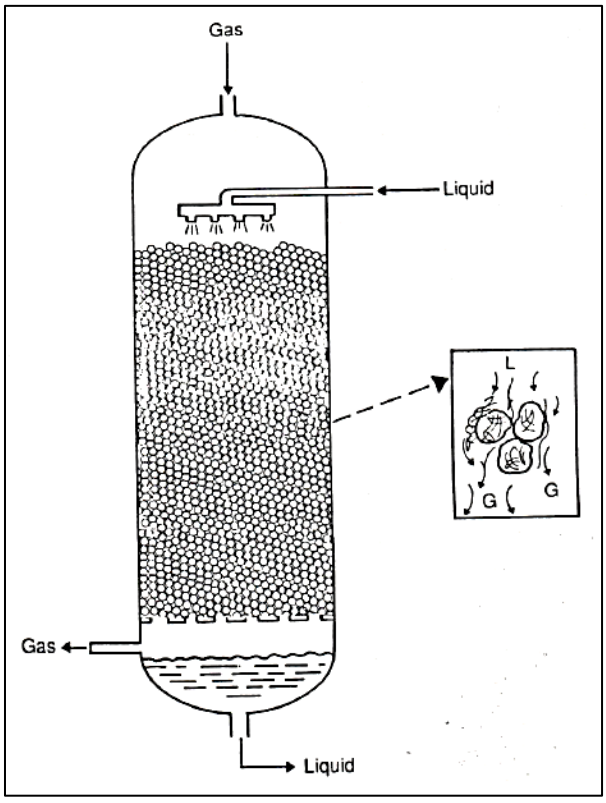

Figure 3: Generic Trickle-Bed Reactor Schematic (Mills et al., 1992)

Flow regime aside, there are several other characteristics of trickle-bed reactors that make this model more applicable to this particular project. In terms of packing, the particles can be inert particles (as is the case for absorption columns) or the particles can be solid catalysts in order to carry out catalytic reactions with three phases. Also, while the gas and liquid phases may be fed countercurrently to the trickle-bed, they may also be fed cocurrently along the channel, similar to the experiments of Vonortas et al. (2010). In addition, achieving plug flow within a trickle-bed reactor translates to more efficient and complete reactions and the lower liquid holdup observed in trickle-beds translates to a decrease in undesired side reactions. An advantage to trickle-bed reactors is the decreased need to handle catalyst particles since these are usually fixed in place within the reactor. Additional advantages include less power loss to the surroundings, ability to operate reactions at higher pressures, lower associated costs, and flexibility with the process and flow configuration variations (Mills et al., 1992).

2.2 Computational Fluid Dynamics (CFD)

The use of computational fluid dynamics was another integral component for the completion of this project since it was the main tool of simulation. In general, CFD is a means to accurately predict phenomena in applications such as fluid flow, heat transfer, mass transfer, and chemical reactions. CFD is computer-based and requires users to follow a general protocol in order to obtain simulation results. The first step is to define a geometry, followed by creating a series of finite volumes that, altogether, make up the whole of the desired geometry. This pattern of finite volumes (or "elements") is referred to as a "mesh" and is typically formed using triangular/quadrilateral elements for 2-D applications and hexahedral/tetrahedral/pyramidal/prismatic elements for 3-D applications. The purpose of the mesh is to allow for the discretization of the Navier-Stokes partial differential equations so that the computer is capable of the computations required. After creating a mesh, boundary conditions and transport properties must be specified as well as any appropriate turbulence models before the user can initialize a solution. Some issues to bear in mind with CFD problems are the need for a fine mesh (small element sizes), the need to attain result convergence prior to analysis, and the need to use appropriate transport and physical properties in the simulation. CFD is a popular tool for solving transport problems because of its ability to give results for problems where no correlations or experimental data exist and also to produce results not possible in a laboratory situation. CFD is also useful for design since it can be directly translated to a physical setup and is cost-effective (Bakker et al., 2001).

The following two sections summarize basic CFD concepts as they relate specifically to multiphase flow modeling and the advantages to using CFD for multiphase flow simulations.

2.2.1 Fundamentals of CFD for Multiphase Flow

Multiphase flow modeling with CFD poses a couple of challenges that are unique to this type of problem. The first obstacle is dealing with the interactions between phases; this is termed "coupling", and the chosen coupling scheme alerts the program how to treat the phases in the flow. Table 3 below describes the three different coupling schemes available in CFD programs:

Coupling Scheme	Description
One-way coupling	Primary phase affects flow of secondary phase, secondary phase does NOT affect flow of primary phase
Two-way coupling	Primary phase affects flow of secondary phase, secondary phase affects flow of primary phase, particles of secondary phase do NOT interact with one another
Four-way coupling	Primary phase affects flow of secondary phase, secondary phase affects flow of primary phase, particles of secondary phase interact with one another

Table 3: Summary of CFD Coupling Schemes (Andersson, et al., 2012) (Bakker, Computational Fluid Dynamics Lectures: Lecture 14. Multiphase flow, 2008)

The other important issue to address when using CFD to model multiphase flow is how to choose a multiphase model that will be used to compute solutions. An appropriate selection must be made for the multiphase model to ensure that the program is able to utilize the correct continuity equations and also apply them to the fluids in a way that most accurately mimics real-life fluid flow. There are several types of multiphase models and each exhibit a different level of complexity. The multiphase model types, in order of increasing complexity and with brief descriptions, are as follows:

1) *Lagrangian Model*: Continuity equations are solved for the primary phase as the whole entity while individual particles from the secondary phase are tracked throughout the flow and are assumed not to interact with one another.
2) *Algebraic Slip Model*: Primary and secondary phases are treated as one composite mixture and one momentum equation is solved for the combined phases.
3) *Eulerian-Eulerian Model*: Primary and secondary phases are treated individually as being continuous and separate momentum equations are solved for each phase.
4) *Volume of Fluid (VOF) Model*: An Eulerian-Eulerian variation in which the secondary phase is not dispersed within the primary phase but rather there is an interface between the phases and so the interface must be tracked while also solving a momentum equation for each phase.
5) *Discrete Element Method*: The most complex multiphase model in which momentum equations are applied to individual particles of the secondary phase as well as to the primary phase as a whole.

(Bakker, Computational Fluid Dynamics Lectures: Lecture 14. Multiphase flow, 2008), (Andersson, et al., 2012)

Each multiphase flow model has applications for which it is best adapted depending on the typical flow regime present in a particular multiphase flow system. The most commonly used multiphase models are the algebraic-slip model and the Eulerian-Eulerian/VOF models. Table 4 below gives examples of these multiphase model types and physical systems that can be simulated with these types of models:

Multiphase Model	Applications
Algebraic-slip model	Bubble column design, gas-liquid mixing vessels
Eulerian-Eulerian/VOF model	Fluidized bed systems, which encompass catalytic reactions such as hydrocarbon cracking and non-catalytic reactions, both homo- and heterogeneous

Table 4: Some Common Uses for CFD Multiphase Models (Bakker, Computational Fluid Dynamics Lectures: Lecture 14. Multiphase flow, 2008)

There are a variety of CFD programs available that possess these capabilities for modeling multiphase flow. Some common programs include ANSYS and COMSOL, which are both multiphysics modeling software packages, and FLUENT, which is a fluid-flow-specific software package. ANSYS version 13.0 was chosen for this project, which will be discussed in further detail in the Methods chapter of this report. For all of these programs, a general protocol is followed in order to obtain the desired results from a fluid flow problem; this protocol is the same as the general CFD principles described earlier in this section except for the type of fluid flow (i.e. multiphase). First, the geometry must be defined to provide the program with the volume through which fluid will be flowing. CFD programs have the capability to define geometry; however it is also possible to use an outside modeling software package (such as SolidWorks) to create geometry that can then be imported into a CFD program in the event that the user has more expertise in an outside modeling program or would be able to simplify the creation of complex geometries. Next, the geometry must have a mesh applied to it, which is (in simplest terms) a division of the geometry into discrete elements that the program will use to iterate the equations of continuity and momentum. Once the mesh has been applied, a solution method must be defined, which will indicate to the program how to apply the equations of continuity and momentum, which assumptions about the flow should be made, and how many iterations to complete to find a solution. The final step is to allow the program to calculate a solution and then analyze the results.

Chapter 3: Methods

The goal of this project was to complete a two-phase flow dispersion simulation for the horizontal string reactor described by Vonortas et al. (2010) in order to compare the results obtained from the CFD simulation to the experimental results reported. The steps taken to reach this goal are delineated in the following sections of this chapter.

3.1 Model Geometry

Determining the model geometry was the first step towards solving the two-phase flow problem. While some specifications for the geometry were already given by Vonortas et al. (2010), other specifications had to be made based on assumptions related to the capabilities of ANSYS 13.0.

3.1.1 Specifications

Vonortas et al. (2010) specified a catalytic reactor geometry called the horizontal string reactor. This model geometry consisted of a square channel laid horizontally that was constructed from poly(methyl methacrylate) (PMMA) and packed with spherical particles. The channel dimensions reported were a cross-sectional area of 16 mm^2 and a length of one meter. The spheres used for packing were solid, non- porous, and made of glass with a reported diameter of 2.9 mm. Vonortas et al. (2010) described the packing in the following manner: "…the packed spheres were mostly laying at the bottom of the channel with the minority of them at the top." No report was made to address the conditions present at the ends of the channel to keep the particles in place. Additionally, the void fraction, or porosity, was reported as 0.64 and was represented by ε. This value was determined based on experimental results for liquid water alone in the packed channel and can be described by the following equation:

$$\varepsilon = \frac{Q_L}{u_L A_R}$$

In the above equation, Q_L was defined as the liquid volume flow rate, u_L was defined as the actual mean liquid water velocity, and A_R was defined as the cross-sectional area of the reactor. In essence, the equation demonstrates that the volume of water flowing through the channel was divided by the total volume of water that would have been flowing through the channel if the channel were empty to obtain the void fraction (Vonortas et al., 2010). The void fraction is best defined as the percentage of a packed channel that is available for free fluid flow. A simpler way of defining void fraction is to take the volume of the channel not occupied by spheres and divide by the total volume of the channel as if it were empty. This relation can be seen in the following equation:

$$\varepsilon = \frac{V_{tube} - V_{spheres}}{V_{tube}}$$

3.1.2 Creating Idealized Test Models

Since the model geometry description from Vonortas et al. (2010) lacked details for the specific placement of spherical particles in the channel, and also since a random packing (such as the one described in the quote above) could not be replicated accurately, a series of idealized packing models were chosen to test in ANSYS 13.0. These models were designed in SolidWorks based on the channel

and sphere dimensions reported by Vonortas et al. (2010) in addition to calculated sphere origins (tabulated calculations of these origins can be seen in Appendix A). Verification of the orientation of packing was tested in a laboratory using a scale model of the spheres and channel to observe that particles packed in the preferred manner.

The first model can be described as the diagonally-packed channel, in which spheres were placed alternately in a bottom corner of the channel and then in the opposite upper corner to create the "string of particles" described by Vonortas et al. (2010). This model geometry demonstrated two corners of the channel that were empty upon completion of packing; these corners were the two not occupied by spheres. Physical packing can be observed in Figure 4 below:

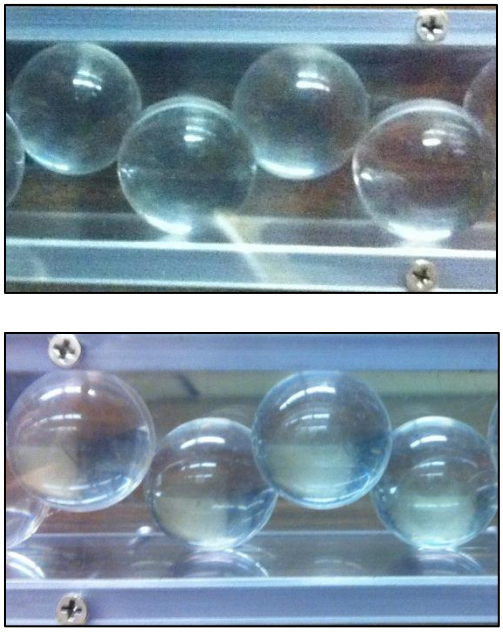

Figure 4: Diagonally-Packed Channel Physical Packing. Above: Side View. Below: Top View.

The second model can be described as the bottom-packed channel, in which spheres were placed along the bottom of the channel in a zig-zag pattern to leave open space along the top of the channel above the spheres. Physical packing can be observed in Figure 5 below:

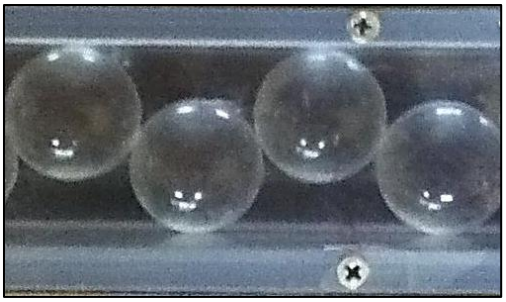

Figure 5: Bottom-Packed Channel Physical Packing. Above: Side View. Below: Top View

The third model can be described as the spiral-packed channel, in which spheres were packed in a clockwise spiral relative to the inlet inside the channel. Physical packing can be observed in Figure 6 below:

Figure 6: Spiral-Packed Channel Physical Packing. Above: Side View. Below: Top View.

These models were chosen for testing because they exhibit differences in the amount of free-channel space for fluids to flow through. These models were also chosen because they exhibit repeating particle packing structures that are similar to the packing of Vonortas et al. (2010) but less ambiguous because each sphere placement is known exactly.

3.1.3 Optimizing Test Models

After selecting model geometries to work with, the diagonally-packed channel was the first SolidWorks file to be imported into ANSYS 13.0 for meshing. The diagonally-packed channel was chosen because it was one of two geometries that closely resembled the geometry specified by Vonortas et al. (2010). Meshing initially failed due to the contact points between spherical particles, or the point at

which the surfaces of two spheres touch. In these areas, the elements of the mesh became infinitely small in order to accommodate the decrease in area around the contact points. This consequently led to meshes with so many elements that the program was unable to handle such a large mesh.

Several possible solutions to the contact point issue were considered. One possibility was to maintain the same sphere origins while increasing the size of the spheres enough for the spheres to overlap with the walls and each other, hence eliminating the singular contact point between surfaces. The enlarged spheres were increased in volume by multiplying the volume by a factor of 1.0150, which made the overlap between spheres equal to one-twentieth of the diameter of the sphere. This idea is illustrated in Figure 7 below:

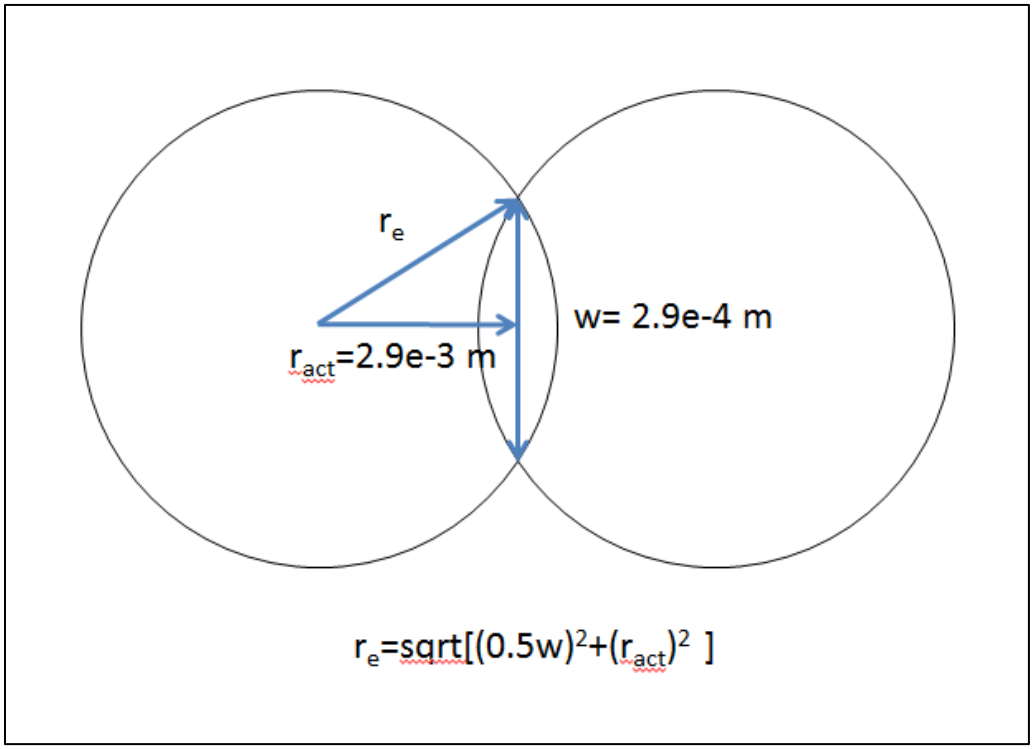

Figure 7: Determining increase in sphere diameter for enlarged particles

Another possibility was the converse to this solution, in which sphere origins were again maintained but the spheres were decreased in size enough to ensure that the spheres did not actually contact another surface. The reduced spheres were decreased in volume by multiplying the volume by a factor of 0.9851, which made the gap between spheres equal to one-twentieth of the diameter of the sphere. In other words, the diameter of the reduced sphere was decreased by the same amount that the enlarged sphere diameter was increased by. A third possibility was to create bridges at the contact points, or small cylinders between spheres that encompassed the contact points and therefore eliminated the single contact point issue. The bridges in question were designated as having a diameter that was one-tenth the diameter of a spherical particle; this size was based on common practice in CFD solutions. The overall volume of the bridged spheres was 1.0001 times the volume of the spheres without bridges.

In the end, the bridge option was chosen as the best solution to the contact point issue. This was based on the concept of void fraction, which was discussed previously as being the percentage of a packed channel that is available for free fluid flow. The bridge option was the solution that altered the void fraction the least, which was important for maintaining as much similarity as possible to the physical experiment performed by Vonortas et al. (2010). Calculations to determine the placement of bridges can be seen in Appendix A. A comparison of void fractions for each possible contact point solution can be seen below in Table 5, while a sample calculation for calculating void fraction can be seen in Appendix B:

Contact Point Solution	Diagonally-Packed Channel Void Fraction (408 particles in 1 meter)	Bottom-Packed Channel Void Fraction (372 particles in 1 meter)	Spiral-Packed Channel Void Fraction (372 particles in 1 meter)
Ideal Channel (exhibits contact points)	0.6744	0.7031	0.7031
Enlarged Spheres	0.6695	0.6986	0.6986
Reduced Spheres	0.6792	0.7075	0.7075
Bridged Spheres	0.6743	0.7031	0.7031

Table 5: Comparison of Void Fractions for Possible Contact Point Solutions

The final models incorporated the bridges and sections of the models can be seen below in Figure 8, Figure 9, and Figure 10. Each figure shows an inlet and side view of the models with the side views exhibiting all hidden edges to better observe the placement of bridges.

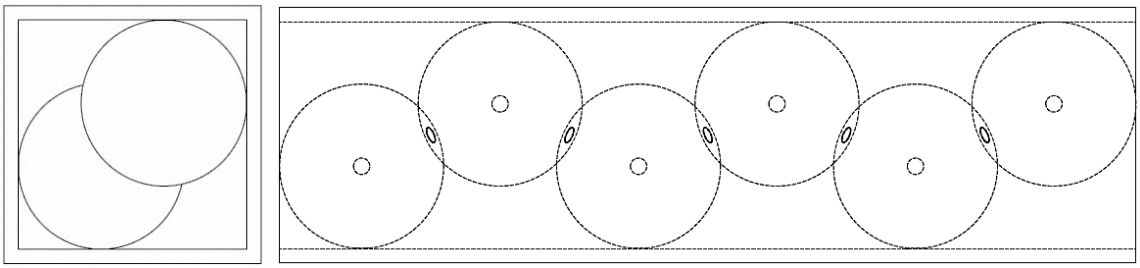

Figure 8: Diagonally-Packed Model with Bridges, Inlet and Side Views

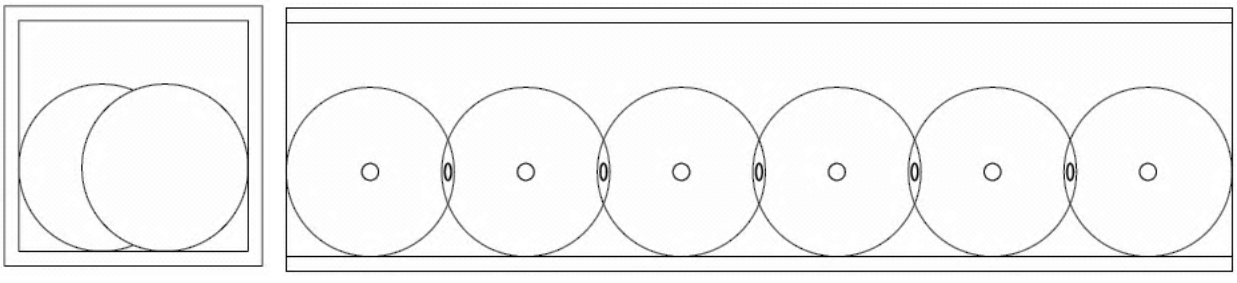

Figure 9: Bottom-Packed Model with Bridges, Inlet and Side Views

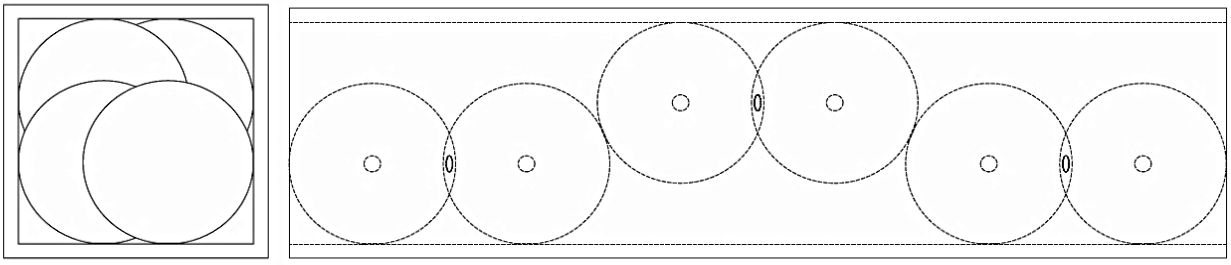

Figure 10: Spiral-Packed Model with Bridges, Inlet and Side Views

Several varieties of each model were made for the purposes of simplifying the model for the CFD program's computations. The first variation was an empty channel with the same cross-sectional dimensions as the packed channels and a length of 10cm (one-tenth of the specified length). This model was created for a series of preliminary tests that would provide supporting evidence to the end results on multiphase flow in packed channels. The second model variation was a four-sphere model for each geometric configuration discussed above (three 4-sphere models total). These models were purposely kept at approximately one-hundredth of the actual channel in order to allow for quick generation of results when trying to obtain a general idea of how a certain solution setup would work. The final model variations were a 40-sphere model for the diagonally-packed channel and a 36-sphere model for the bottom- and spiral-packed models. These models were constructed for the purposes of examining flow over a longer section of particles while still keeping the total solution time to a relative minimum.

3.1.4 Mesh Preparation

The final order of business before moving on to the next step towards reaching the project goal was to take the optimized model geometries from SolidWorks and import them into ANSYS so meshing could begin. Models were imported as ACIS (.sat) files, which was the geometry file from SolidWorks that was compatible with ANSYS. Once imported, the geometry could be used to define the volume through which fluid flow would be occurring. This was accomplished by inverting the SolidWorks geometries to leave behind the fluid, or void, space. In other words, the geometry acted as a mold for creating the volume. The inversion was completed by creating faces, or caps, at each end of the channel, filling the void space, and then removing the original solid parts. Once the void space was obtained, the model was ready to have a mesh applied to it.

3.2 Meshing

Determining a mesh was the second step towards solving the two-phase flow problem. The following sections describe the various parameters of the mesh that needed to be selected and how each parameter was chosen.

3.2.1 Mesh Basics

The 10cm empty channel was used as the geometry basis for creating a mesh and later calculating a solution in ANSYS. This shorter section was analyzed at first to decrease the time required by the program for meshing and iterating a solution. Focusing on a short section of the channel also made it easier to visually analyze the meshes created as well as to inspect the solution. The geometry for the one-meter long diagonally-packed channel (previously described) was originally used to try and

create a mesh since this model had been identified as being closely related to the physical geometry of Vonortas et al. (2010). Due to the complex geometry of the packed channel and the resulting complications associated with creating a mesh, the 10cm empty channel was then meshed and analyzed in order to determine an appropriate mesh to apply to the packed channel. The different parameters presented in the ANSYS Meshing program could then be examined in more detail if this simpler geometry was used as a basis. Eliminating the packing provided clarity for situations in which mesh specifications were not uniform throughout the channel or were not applied throughout the channel. Once a simpler model was chosen to be used for mesh refinement, the actual process of systematically specifying mesh parameters as well as understanding the ANSYS Meshing program was accomplished. The following sections on creating a mesh are based solely on the empty channel and its experimental meshes that led to the final mesh that was to be applied to the packed channel.

3.2.2 Mesh Parameters

Different mesh options were further analyzed using the empty square channel. The standard mesh parameters can be separated into six categories: default, sizing, inflation, cut cell meshing, advanced options, and defeaturing. Due to the nature of the geometry in question, cut cell meshing and defeaturing were not changed from the default settings which included no active cut cell meshing and automatic mesh-based defeaturing. Similarly, there was no need to explore advanced options, so this category remained untouched.

The default category included Physics Preference, Solver Preference, and Relevance. The Physics Preference was CFD (Computational Fluid Dynamics) due to the project goal specification that CFD be performed. FLUENT was chosen as the Solver Preference for reasons similar to the choice that led to using CFD as the Physics Preference. ANSYS is a multiphysics program that can be used for many types of systems (including many mechanical problems) and it has several solver components to address the needs of these different types of systems. The fluid flow problems, similar to the one in this project, are best solved by FLUENT CFD. Relevance qualitatively defines the fineness of the mesh and incorporates additional quantitative conditions that need to be specified. The ANSYS Meshing software defines a scale from -100 to 100, with zero being the “moderate” mesh size. Further constraints were added later to define the quantitative mesh size after this step, so the Relevance was set at zero as a base point.

The Sizing category was mainly kept as the given default conditions. The two main differences included turning off the Advanced Sizing Features for the empty channel and specifying the Relevance Center as Fine. The advanced sizing features added complexity to the problem that was not needed and resulted in a less-uniform mesh overall. The Relevance Center was specified as “fine” to increase the uniformity overall. Mesh uniformity was important for this project because meshes with high uniformity can be used to calculate more accurate results.

The Inflation category specified the transition from the fluid at the wall to the fluid in free flow towards the center. The Inflation Layers specified in ANSYS were similar to boundary layers found in other meshing programs. The layers were made of quadrilateral elements, unlike the tetrahedral and hexagonal elements present in the body of the model. The boundary layer elements were also smaller in

size than the average body element size. The Boundary Layers allowed the computer to use no-slip boundary conditions near the walls where the change in velocity gradient is drastically different than throughout the center of the body. Boundary layers were important for this project because of the greater rate of change in flow parameters present at the walls as well as the anticipated viscous effects at the walls due to the laminar flows of both components in the channel.

Inflation for the empty square channel was created on the walls of the channel. Inflation details can be specified by a number of options in the ANSYS Meshing Program. The options include Total Thickness, First Layer Thickness, Smooth Transition, First Aspect Ratio, and Last Aspect Ratio. The two options that were pertinent to this project were Total Thickness and First Layer Thickness. Both options required the total number of layers, the growth rate, and the inflation algorithm to be specified. The total number of boundary layers is one of the options that can dramatically affect the solution of the problem and the resulting data. With this in mind, the total number of layers was chosen by a guess-and-check method involving different simulations where the number of boundary layers was varied to see the effect on the solution. The same technique was used to determine the estimated total thickness of the inflation layer. The growth rate function was not used and was set at one which resulted in uniform inflation layer thickness. The inflation algorithm was specified as “pre” because this was most compatible with external sizing constraints, body sizing and match control on the system, which will be explained in detail later in this section. The Advanced Options were not changed at all. Collision Avoidance, which was very important for the packed channel, defaulted to Layer Compression; this was the required setting in order to deal with the given geometry and gaps presented by the bridges. An example of Layer Compression can be seen in Figure 11 below:

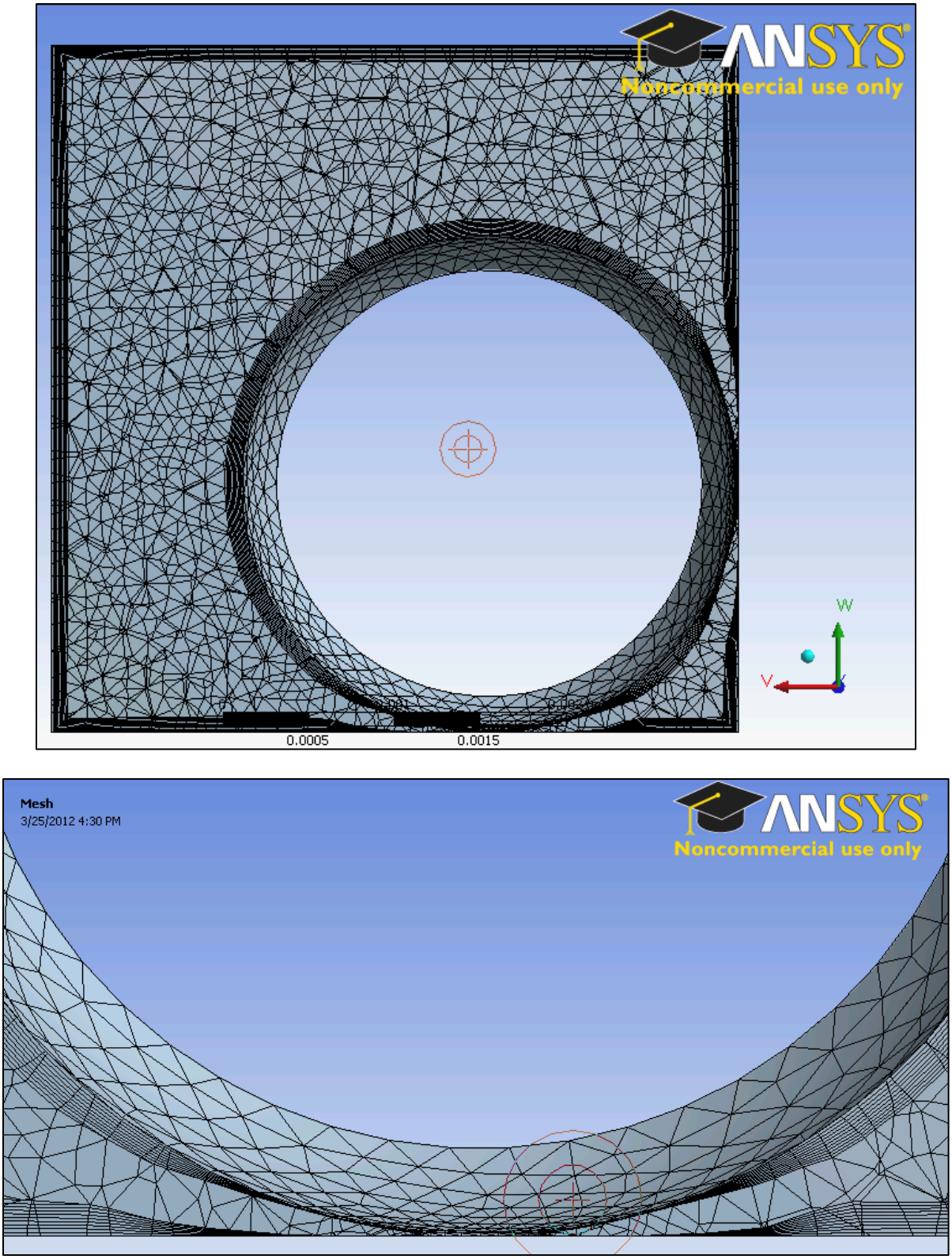

Figure 11: Example of Layer Compression. Above: Cross-section of sphere close to walls. Below: Close-up view of gap between sphere and wall.

3.2.3 External Sizing Constraints

Two external constraints applied to the mesh were not a part of the initial default specifications that were required by the ANSYS Meshing Software. These constraints were Match Control and Body Sizing. Match Control is an external constraint applied to faces that results in identical meshes on two different surfaces. This constraint is necessary if a periodic boundary condition will be specified in the FLUENT portion of the problem. In the case of this project, it was anticipated that a periodic boundary condition may need to be specified in order to decrease solution time by decreasing the length of channel necessary to be solved (this will be further discussed in an upcoming section). Match Control was also necessary in order to later apply periodic conditions in the FLUENT section because this allowed for entry and exit lengths on the channel to be omitted. The Body Sizing constraint is a refinement placed on the whole of a solid, which in this case was the channel. Body Sizing results in a uniform mesh (consistent element sizing) and is applicable in a geometry that would require high mesh consistency to solve properly. Body Sizing was necessary in order to obtain the desired highly uniform mesh throughout the fluid flow volume because the spherical particles provided a challenge to the program to generate the desired mesh without the body sizing. The other options for overall mesh constraints were Face Sizing and Edge Sizing; Figure 12 through Figure 20 below demonstrate the variance in mesh uniformity between mesh types:

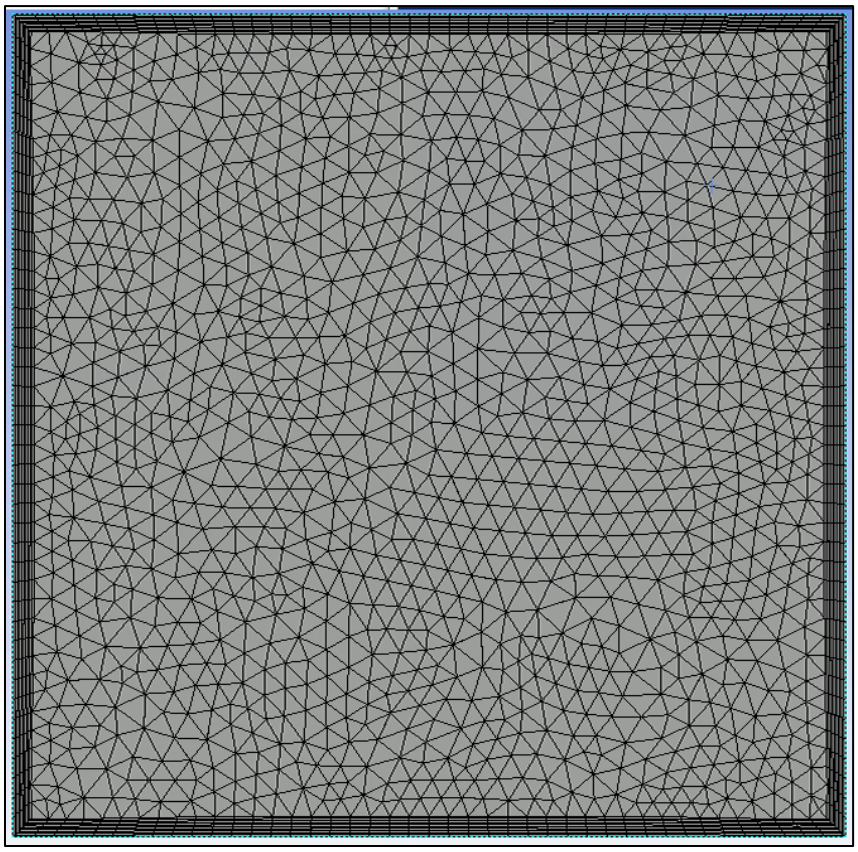

Figure 12: Example of face sizing mesh, inlet view.

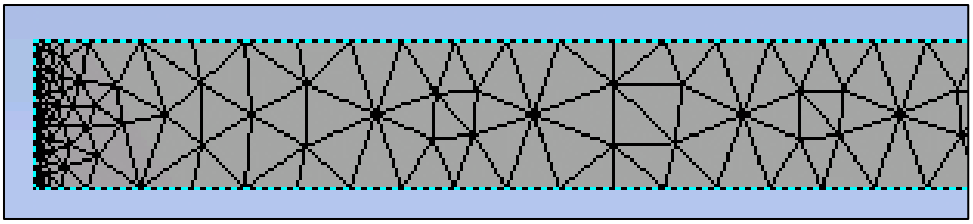

Figure 13: Example of face sizing mesh, side view of one end.

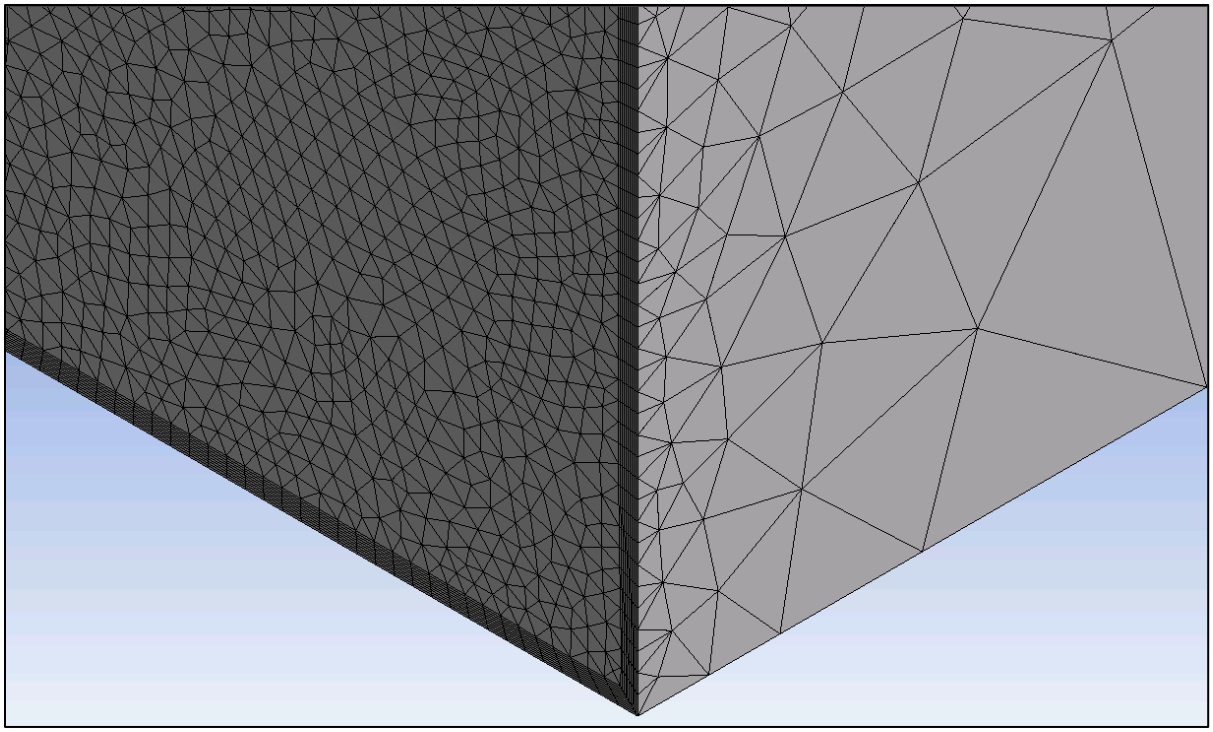

Figure 14: Example of face sizing mesh, partial isometric view of inlet.

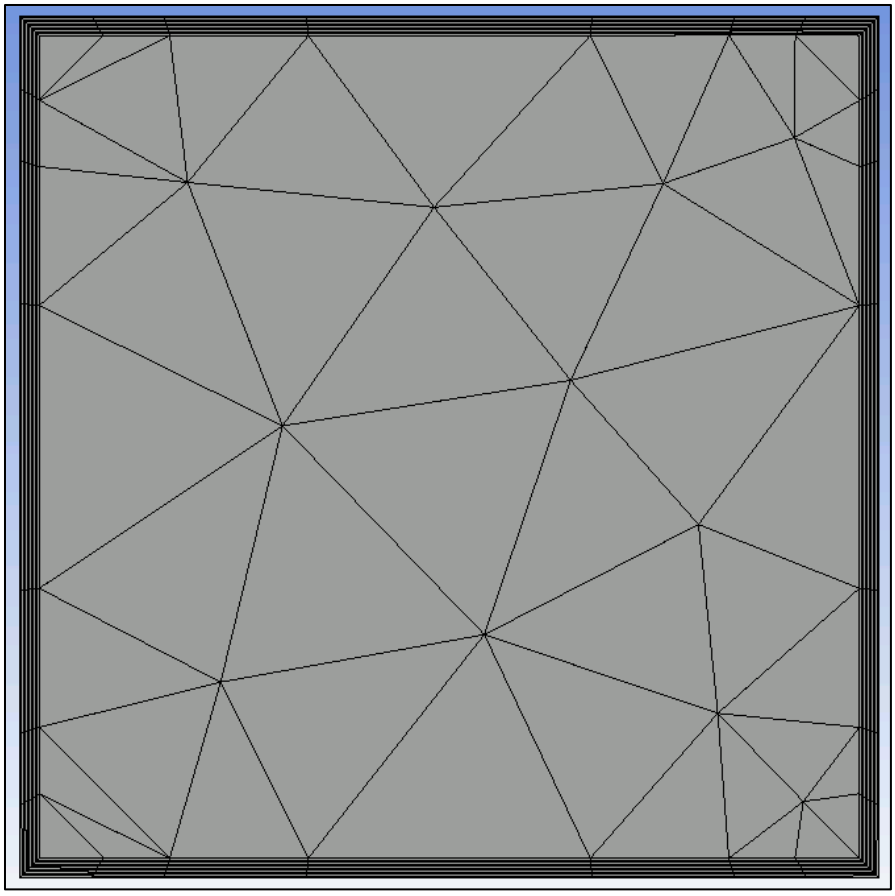

Figure 15: Example of edge sizing mesh, inlet view.

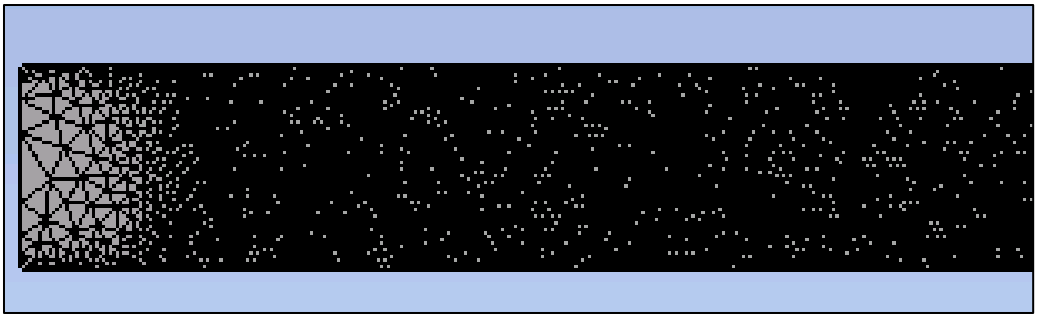

Figure 16: Example of edge sizing mesh, side view of one end.

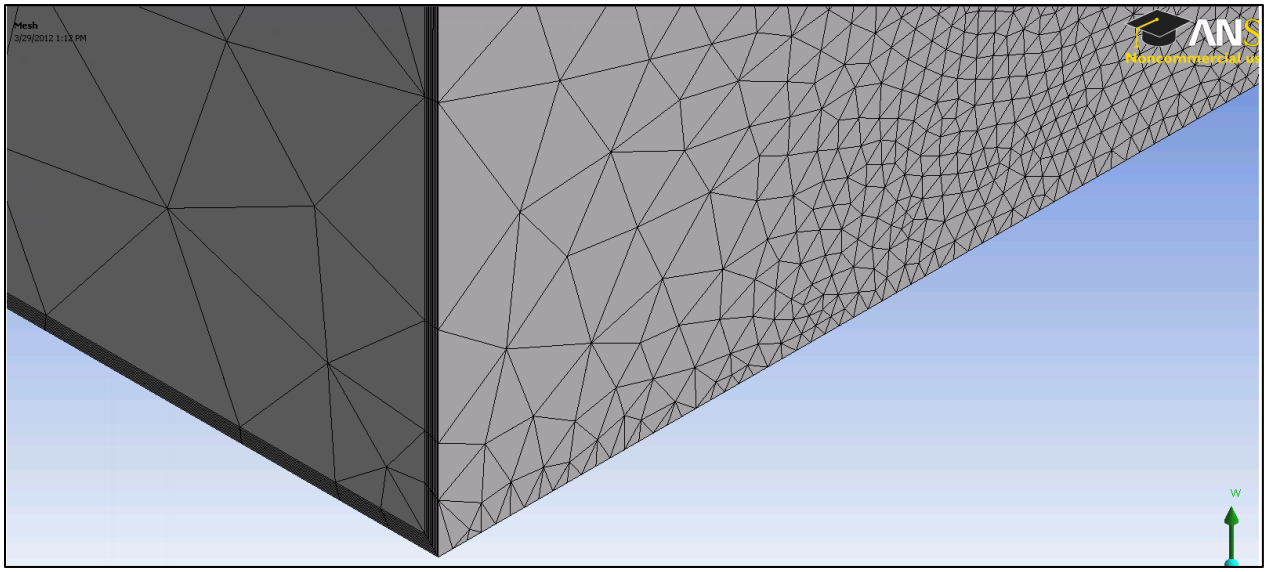

Figure 17: Example of edge sizing mesh, partial isometric view of inlet.

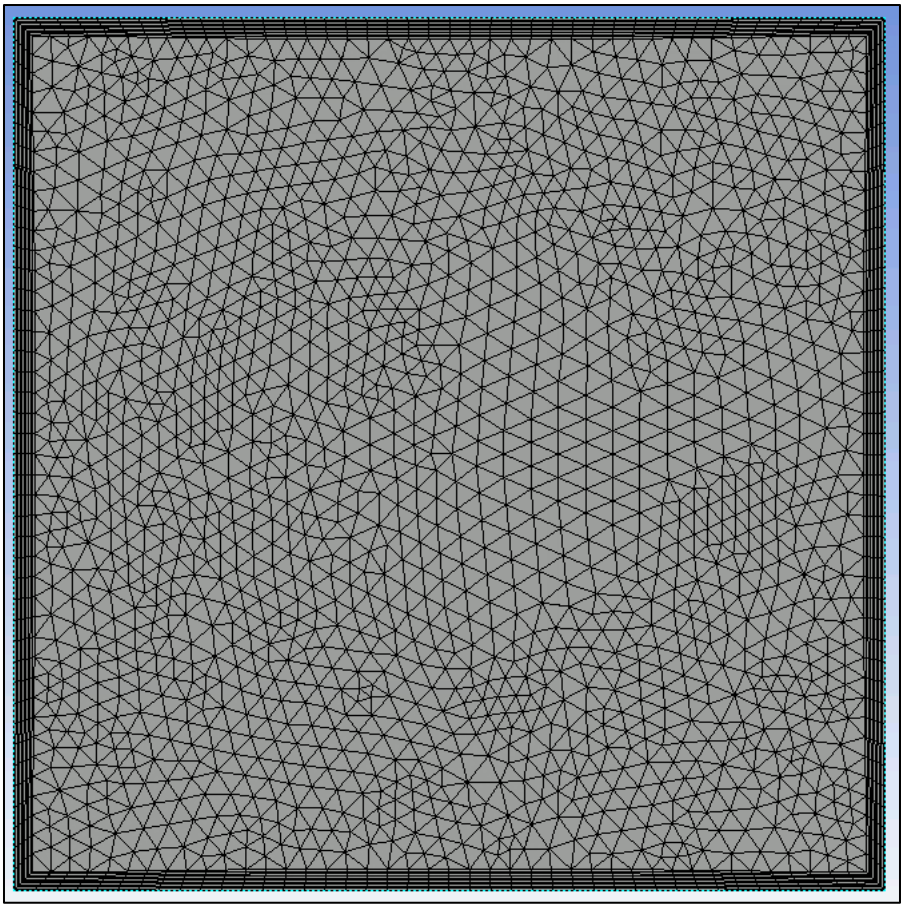

Figure 18: Example of body sizing mesh, inlet view.

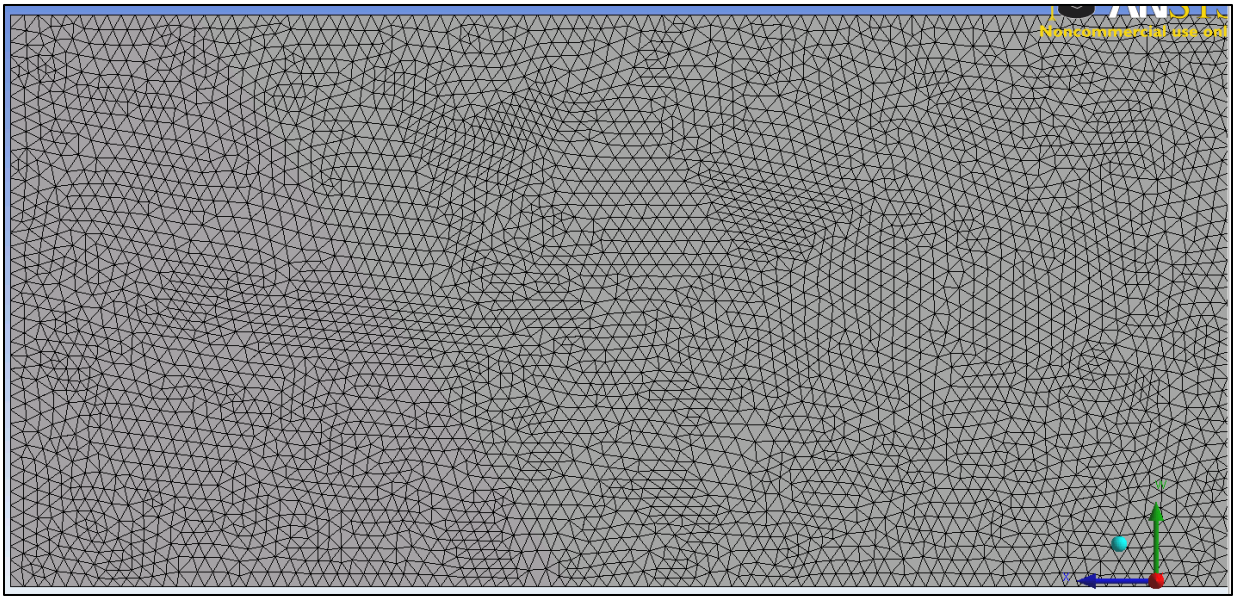

Figure 19: Example of body sizing mesh, side view of one end.

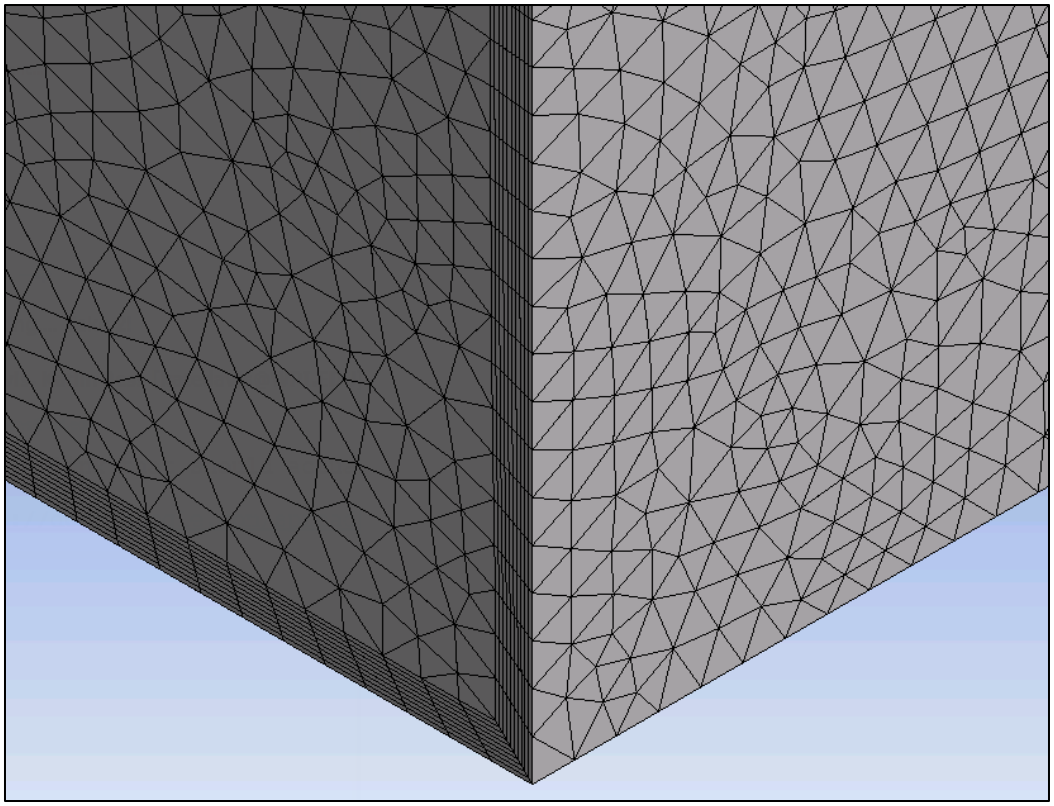

Figure 20: Example of body sizing mesh, partial isometric view of inlet.

3.2.4 Body Sizing

The parameters for Body Sizing were Type, Element Size, and Behavior. The element sizing of the mesh required uniformity so the Element Size option was activated and further specified. The

element sizes were chosen to be proportional to the diameter of the spherical particles based on common practice in CFD experimentation. Typical element sizes for packed beds were on the order of a twentieth of the particle diameter, or $D_p/20$. Other element sizes that were examined included $D_p/30$, $D_p/40$, and $D_p/50$. Behavior dictated how flexible the program could be with the sizing of the mesh. The overall sizing control was used as a maximum size constraint for this project and resulted in Soft Behavior. Soft Behavior allows the program to alter the body sizing to accommodate other specified parameters that take precedence in meshing.

3.2.5 Match Control

To apply a Match Control to the mesh, two faces were selected which exhibited identical geometry and topology. Arbitrary Transformation was specified which demanded that a coordinate system be specified on each surface. Once the Match Control was applied, it guaranteed that the mesh on both faces was exactly the same.

3.2.6 Final Mesh Specifications

The empty channel was used to determine the final mesh for the packed channels due to previously established pressure drop correlations for empty channels. The calculated pressure drops resulting from the correlations and the pressure drop reported by ANSYS FLUENT could then be compared for program accuracy; the mesh was then refined further to increase the accuracy of the pressure drop from ANSYS FLUENT in comparison to the calculated pressure drop. This mesh-testing technique was used most for the 10cm empty channel with single-phase flow; however, the same technique was applied for multiphase flow in the 10cm empty channel and single-phase flow in a packed channel to verify that the chosen mesh was performing appropriately. Sample calculations for finding the pressure drop for each of the above-mentioned situations can be seen in Appendices C, D, and E.

The final mesh applied to the packed models had a body size constraint of $D_p/30$ with match control on the inlet and outlet surfaces and 10 Inflation Layers with a total thickness of $1x10^{-4}$ meters. The chosen body size was a compromise between the program's ability to generate such a fine mesh and the accuracy of results that accompanies smaller mesh sizing. Mesh sizes of $D_p/40$ and $D_p/50$ resulted in too many elements and nodes which meant a very long solving time in FLUENT. A mesh size of $D_p/20$ resulted in high error in the FLUENT solution. The balance between error and program capability was the reason for choosing the mesh size of $D_p/30$. Figure 21, Figure 22, and Figure 23 below provide a visual aid for the completed mesh; an isometric view of the channel inlet as well as a frontal view of the inlet and a side view are pictured:

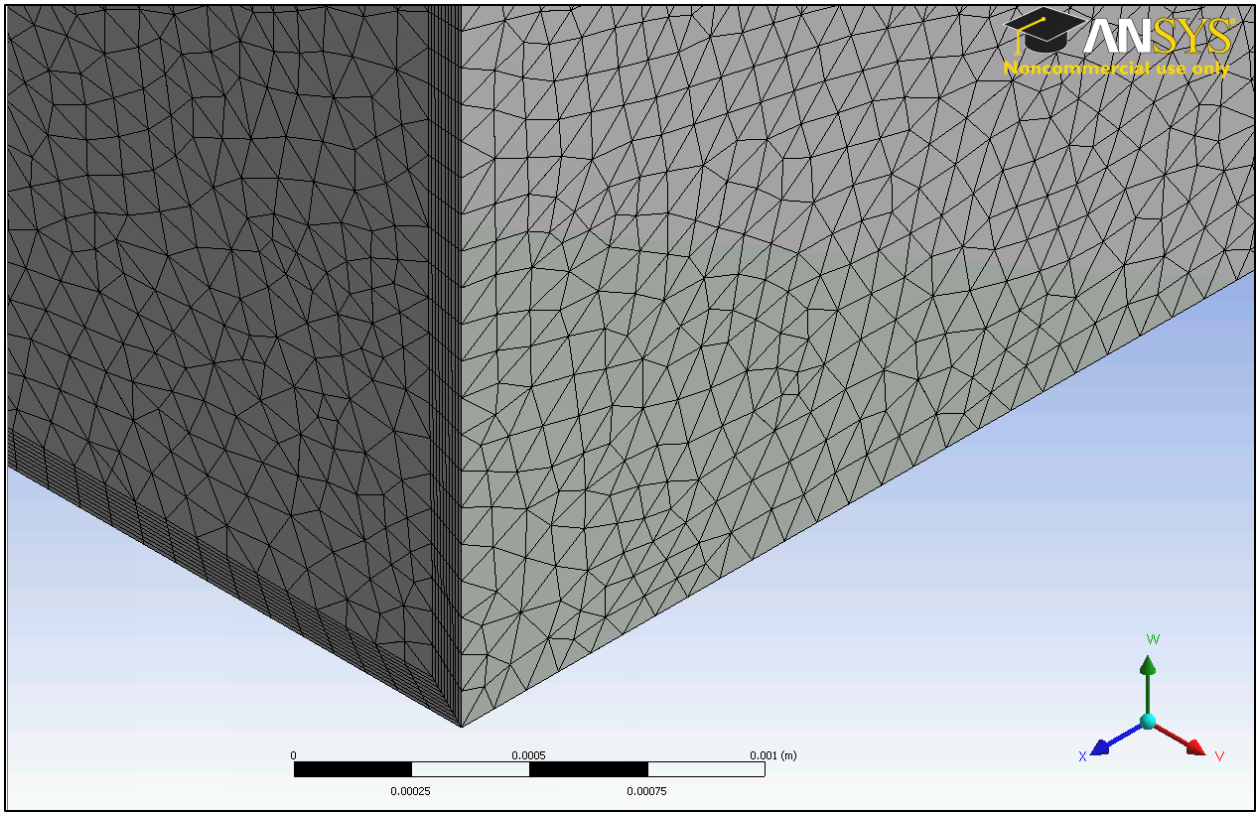

Figure 21: Isometric View of Mesh at Channel Inlet, Bottom Corner

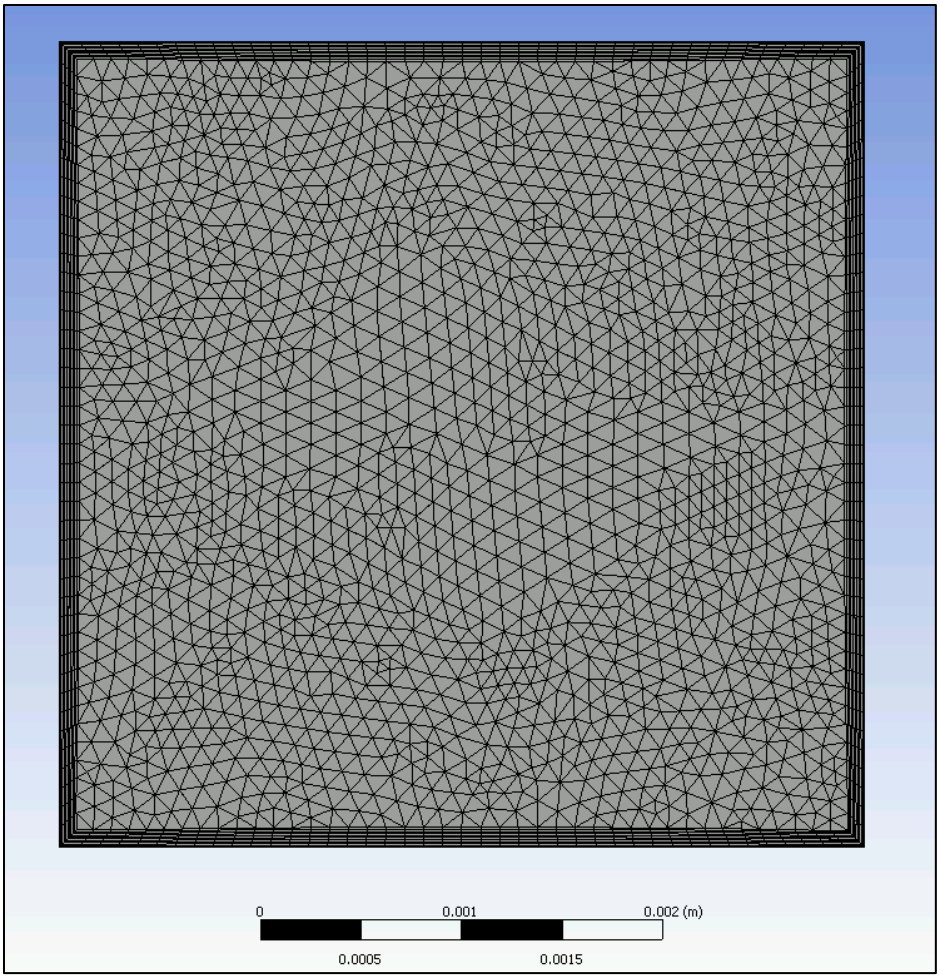

Figure 22: Frontal View of Mesh at Channel Inlet

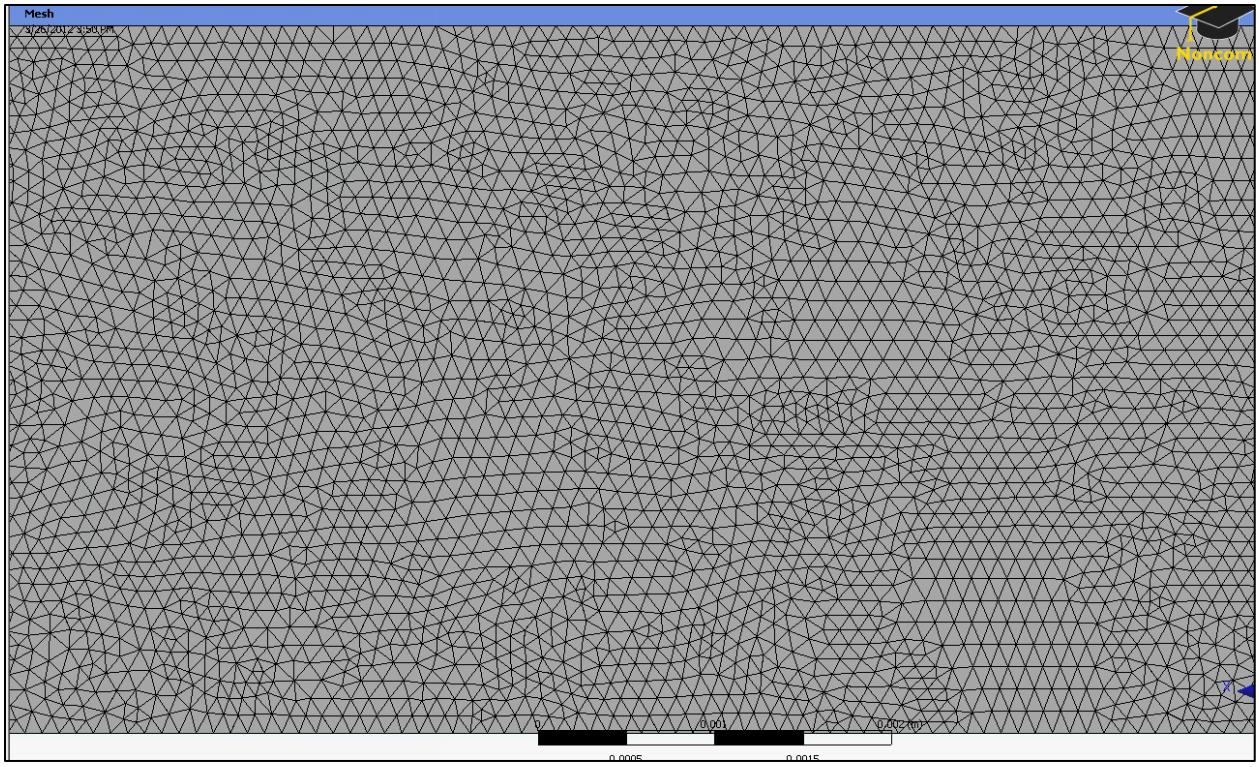

Figure 23: Partial Side View of Final Channel Mesh

3.3 Solution of Model

Initializing the solution of the model was the final step towards solving the two-phase flow problem. The following sections describe the various parameters that had to be specified in order to initialize a solution and how each parameter was chosen.

3.3.1 ANSYS FLUENT Solver Assumptions

A few preliminary specifications were made in order to initialize a solution in FLUENT. Parallel, rather than series, processing was used in order to decrease the solving time in FLUENT. Another external constraint applied to the empty channel tests only was the application of a Periodic Boundary Condition. This condition was applied by entering the periodic boundary code into the command box. This command changed the solving mechanism of the whole system. The theory behind Periodic Flow is to simulate a smaller section of flow in a channel that has reached fully developed flow. As was alluded to within a previous section on Match Control, Periodic Flow eliminates the need for entry and exit lengths and allows for a decrease in the length of channel being solved. These two improvements were helpful because entry lengths required for a shorter section of the channel were longer than the channel itself due to the geometry of the channel and the flow conditions specified. Periodic Flow additionally results in accurate data while only using a fraction of the original channel length; this was desirable because the length of the channel meant that a full-channel mesh would be incredibly large and would take days to solve. Periodic Flow in this case was Translational, and the velocity at the inlet and outlet were identical due to the presence of fully developed flow along the section. All things considered, there was still an observable pressure drop across the channel.

One other general specification involved the velocities for water and nitrogen in the channels. A specific case was chosen from the wide variety of fluid velocities presented by Vonortas et al. (2010) where the water velocity was $5x10^{-5}$ m/s and the nitrogen velocity was $1x10^{-3}$ m/s. These velocities were chosen for consistency during testing so that there would be no confusion about which experimental velocities should be applied. Water and nitrogen were also sometimes specified to have velocities of 0.5 m/s and 10 m/s, respectively, so that flow phenomena were more easily observable while still maintaining a laminar flow regime. For some of the final simulations, water and nitrogen were specified to have velocities of 45 m/s and 35 m/s, respectively, in order to observe changes in the CFD solver when different flow parameters were provided.

The next sections describe the solution initialization portions that were specific to either single phase flow or multiphase flow. A complete list of specifications for both single and multiphase solutions is detailed in Appendix F. A general overview and explanation for selecting the specifications are given in the next sections.

3.3.2 Single Phase Solver Options

Two main general specifications were applied for the overall problem. The solver was considered to be a Pressure-Based solver which used the Navier-Stokes equations of continuity to determine velocities based on pressure. The information provided by Vonortas et al. (2010) was not applicable for the alternative option (a Density-Based solver) because only information on inlet velocities and outlet pressure were supplied. The time was specified as Steady State; this assumption could be made due to the specifications reported by Vonortas et al. (2010). This allowed for the assumption of fully developed flow throughout the system.

In the single phase trials the “Models” category was not applicable; however, this category became important for multiphase simulations because this was where multiple phases could be indicated. The material for the single phase simulation was liquid water. The Periodic Flow Specification made at the beginning of the solution initialization affected the specification of Boundary Conditions in the FLUENT Program. Periodic Boundary Conditions were required, and these included supplying an inlet mass flow rate and the pressure being placed on the whole system. The Solution Methods and Controls were kept at default for single phase flow. By selecting specific Monitors, the pressure could be monitored during solving which helped to avoid premature convergence. Premature convergence was also avoided by changing the Residual constraints. The continuity criteria were changed to $1x10^{-10}$, which drastically reduced the probability of the program converging on its own. Defining the number of iterations under Controls made it possible to observe the trends in pressure and pressure drop during the calculation of a solution, which helped to ensure that a more viable end result was achieved. A Surface Monitor was created to show the average pressure at the inlet throughout the solution process. The resulting graph of inlet pressure was also used to monitor if the problem was close to a final solution. Due to the constraints on the convergence specifications, the number of iterations affected the solution greatly. The Surface Monitor allowed for a visual assessment of whether the current set of iterations would result in a viable solution or if additional iterations were required.

3.3.3 Multiphase Solver Options

Problem Setup for the multiphase problems was very similar to the single phase Setup with a few different options. The first major difference was that Multiphase was turned on in the Models section of Setup. The Eulerian Model for multiphase flow was chosen to dictate the interactions between the two phases in the system based on literature that suggested this would be an appropriate mathematical scheme to utilize for this type of two-phase flow. An implicit scheme was also specified because the problem was deemed to be steady state. Laminar Flow was specified for all models to be consistent with the velocities reported by Vonortas et al. (2010).

The materials were specified as liquid water and gaseous nitrogen per the experiment performed by Vonortas et al. (2010). Multiphase flow also required that a primary and secondary phase be indicated for the system. As was discussed in the Background chapter of this report, the secondary phase is the phase dispersed throughout the continuous primary phase. For this problem nitrogen was considered the primary phase and water was considered the secondary phase. The phase interactions were kept as Schiller-Naumann, which was the default recommended in the Help section of ANSYS FLUENT for this type of problem.

Boundary Conditions similar to the single phase systems were required; the major difference was that each material required its own specifications. The Solution Method selected for the multiphase system was the Multiphase Coupled Method; this is a form of two-way coupling which assumed that the primary and secondary phases affected each other but the particles of the secondary phase did not interact. Monitors and Solution Initialization were the same as for single phase. The Solution Controls for multiphase systems were different than for single phase systems because there were additional categories to address. The default Courant number was used, and relaxation factors were reduced by an average of 0.2 to avoid divergence in the solution.

Chapter 4: Results and Discussion

The following sections first describe the merits and hindrances associated with using ANSYS 13.0 to complete the two-phase dispersion simulation. Following this is discussion on the results of the single and multiphase simulations with regards to the ability to replicate the results of Vonortas et al. (2010) using a CFD simulation.

4.1 Effectiveness of Using ANSYS 13.0

After using ANSYS 13.0 for the duration of this project, a better understanding of the program's benefits and shortcomings for the given problem was obtained. Overall, ANSYS 13.0 was deemed to be a less appropriate choice of CFD program for the given problem than other available CFD programs. Additionally, due to external constraints on the materials available for this project, ANSYS 13.0 was an even less appropriate choice for this project since the research licenses necessary were not as readily available as those for other CFD programs. In the end, ANSYS 13.0 and GAMBIT 2.4.6/FLUENT 6.3.26 were utilized in combination to combat the issues surrounding the use of ANSYS 13.0 for this specific project. Some more specific discussion comparing and contrasting the two programs are detailed in the next sections.

4.1.1 Meshing in ANSYS 13.0 vs. GAMBIT 2.4.6

The first indication that ANSYS might not have been the most appropriate choice for this project stemmed from the meshing capabilities the program presented. In general, the ANSYS meshing software presents the user with many default settings that appear to have been incorporated in order to increase the ease of use. In many ways, these defaults seem to be simplifications made to the meshing software in order to increase the range of applicable models that ANSYS can be used to solved (such as being able to solve both mechanical and fluid-specific problems). While incorporating these defaults lessens the learning curve for ANSYS, it was difficult to obtain a concrete understanding of the meshing options and the full capabilities of the meshing software. Without this knowledge, it was not possible to know whether to change the default settings or not, and there was an overall lower amount of control over the exact mesh specifications.

The default mesh settings were also mostly qualitative, which meant even lesser control of the mesh by the user. In order to make quantitative mesh specifications, one had to explore the advanced options in many of the default categories; this was not immediately obvious during preliminary generations of the mesh. Some quantitative mesh parameters that were embedded in default settings could be found in the inflation, sizing, and match control specifications. For instance, boundary layers could only be specified quantitatively if inflation was selected for the mesh. In addition, the user could not specify a mesh element size unless a specific type of sizing for the mesh was selected (i.e. face sizing, edge sizing, body sizing). Finally, the program would not automatically generate a mesh containing any symmetry unless the user specified match control between two faces of the geometry. Before these stipulations were discovered, it was nearly impossible to create a mesh that met the requirements for mesh fineness and uniformity, which in turn would have had a negative effect on the accuracy of the results.

GAMBIT 2.4.6 is the meshing program that is compatible with FLUENT 6.3.26 and this program was considered on a comparative basis to the ANSYS meshing software throughout the project. In GAMBIT, meshes are built entirely from scratch, unlike ANSYS where the meshes are built generally the same for any geometry until the default settings are changed. GAMBIT allows the user to give quantitative mesh parameters from the very beginning, rather than having to deal with the hassle of backtracking through a series of preset categories. On the other hand, GAMBIT has a much steeper learning curve than ANSYS because the user must fully understand each mesh parameter category and what to specify. However, once the categories are mastered, the user is afforded a great deal more control over meshing than is present in ANSYS.

ANSYS was originally chosen for this project based on the lesser learning curve associated with meshing, however it can be concluded that GAMBIT may have been worth taking the time to learn since generating a mesh that meets project needs would have gone smoother than it did in ANSYS. In the end, meshing in GAMBIT may have saved more time on meshing despite the longer period of time required to learn the program. This is important when examining the effectiveness of a CFD program for solving a two-phase flow simulation since one of the considerations is to observe a decrease in time spent by the experimenter to obtain results (in comparison to laboratory testing).

4.1.2 Solving a Model in ANSYS 13.0 vs. FLUENT 6.3.26

Unlike meshing in both ANSYS and GAMBIT, the solution of a model in ANSYS 13.0 was very similar to solving a model in FLUENT 6.3.26. This was most likely due to the fact that ANSYS FLUENT is simply the most recent version of FLUENT under the ANSYS program interface. A major difference between the two programs was the user interface. ANSYS presented an interface that was user-friendly, including a side bar with drop down navigation under each major category of the solution setup. An example of the interface can be seen in Figure 24 below:

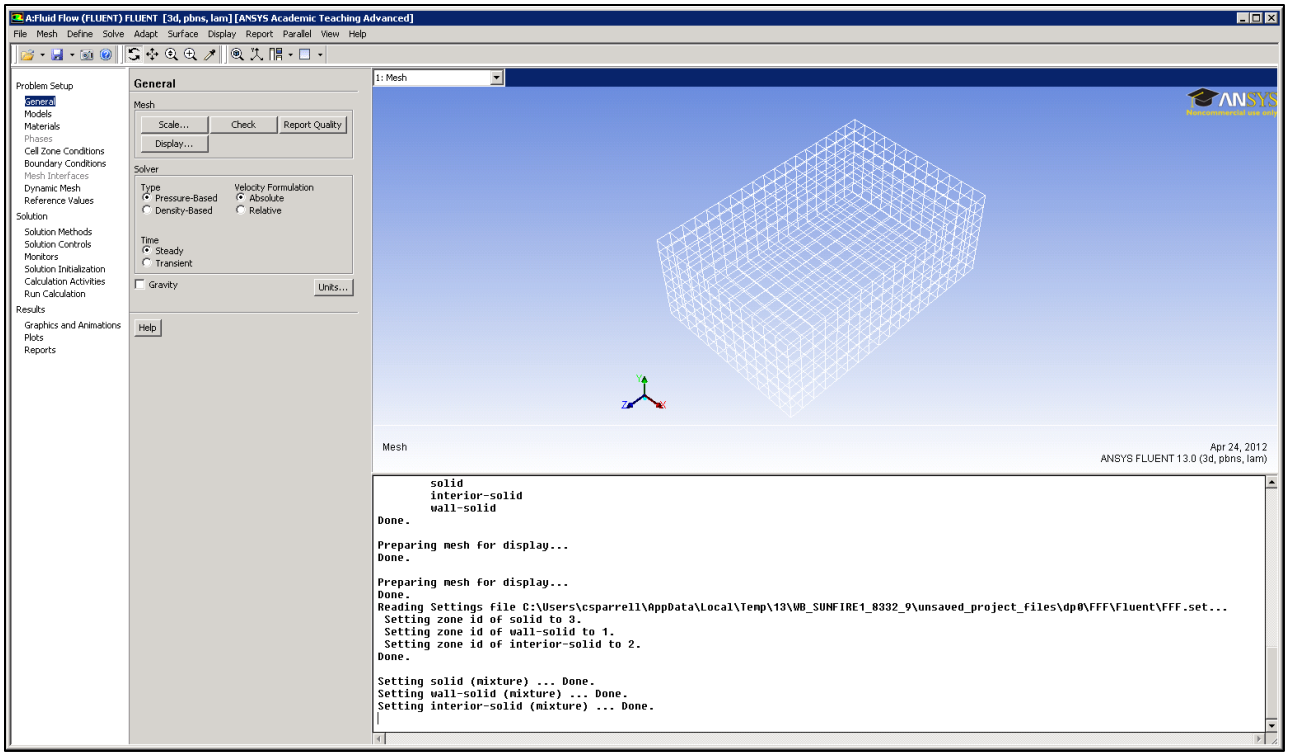

Figure 24: ANSYS 13.0 user interface

FLUENT 6.3.26 presented a less user-friendly interface that was comprised of text boxes, but the categories and parameters were maintained between the two programs. An example of the interface for FLUENT 6.3.26 can be seen in Figure 25 below:

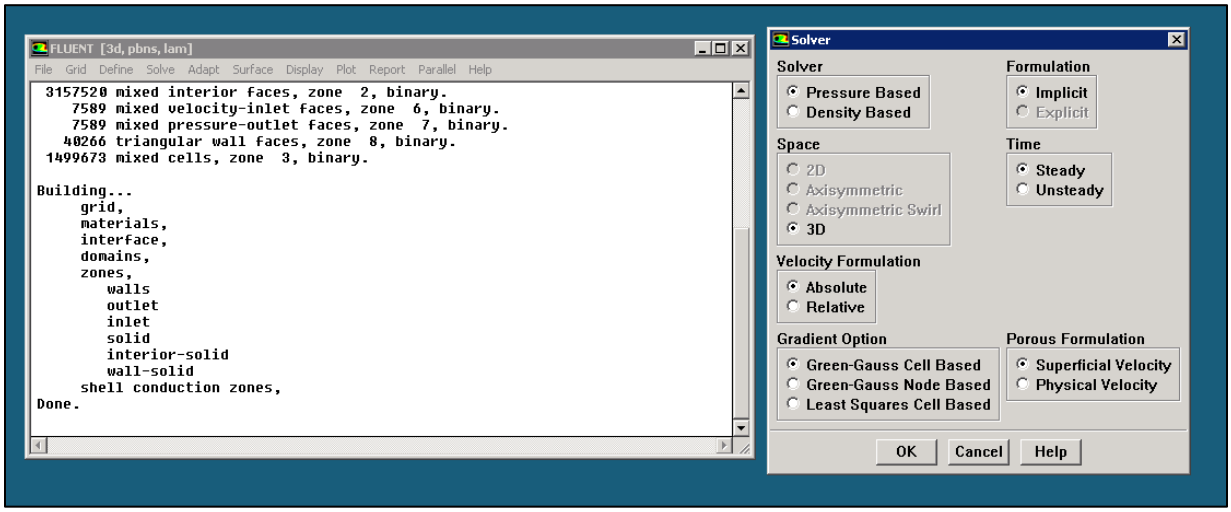

Figure 25: FLUENT 6.3.26 user interface

As mentioned previously, FLUENT 6.3.26 was ultimately used for solving models. This decision was made for a couple of reasons. First, since there was no observable major difference between using ANSYS FLUENT and FLUENT 6.3.26 in terms of time spent with the solution setup, it did not matter

which program was used. Second, there were many unrestricted research licenses available for FLUENT 6.3.26, whereas an unrestricted research license for ANSYS 13.0 had to be purchased and was only available for a limited amount of time. There were many student licenses for ANSYS 13.0 available; however these licenses could only handle solving models with less than 500,000 nodes. Since the models used for this project exceeded the number of nodes allowed by the student licenses, a program with many available research licenses was required. The constraints on using ANSYS to perform solution calculations led to the ultimate use of FLUENT 6.3.26 as the primary solution software since this seemed to be the most practical use of resources in order to work towards other project goals.

4.2 CFD Simulations

Single phase flow in empty and packed channels as well as multiphase flow in an empty channel was simulated in order to lend credibility to the simulations for multiphase flow in the packed channel. These tests were conducted to prove whether or not the multiphase packed channel results were reliable and also to create additional sources besides the results of Vonortas et al. (2010) to determine the percent accuracy of these results. Details of each of these trials can be found in the next sections, and the final section discusses the parameters of interest mentioned in the article by Vonortas et al. (2010) as they were observed in the two-phase flow dispersion simulation.

4.2.1 Single Phase Flow: Empty Channel

Single phase flow in an empty channel was the first set of simulations, as was mentioned previously in the Methods chapter, because this model was meant to prove that the best possible mesh was being obtained and applied to the more complicated problems associated with this project (such as those including packing and additional phases). This conclusion was based on the simulated pressure drop in comparison to a calculated pressure drop and the percent error associated with the simulated value. The 10cm empty channel was used for this set of simulations and periodic boundary conditions were applied to lessen the solution iteration time. Liquid water at 0.5 m/s was specified so that pressure drop would be easily observed. An expected pressure drop was calculated using the Darcy-Weisbach equation, which can be seen below:

$$\Delta P = f * \frac{L}{D} * \frac{\rho V^2}{2}$$

In the above equation, f is the Moody friction factor, L is the length of the channel, D is the diameter of the channel, ρ is the fluid density, and V is the average fluid velocity. When this calculation was first performed, D was substituted with the hydraulic diameter, D_h, to account for the non-circularity of the channel. Additionally, f was determined based on the following relationship:

$$f = \frac{64}{Re}$$

Using this relationship resulted in an expected pressure drop of approximately 1,001 Pa/m for the empty channel.

In order to determine the most appropriate mesh that produced a reasonable pressure drop (within 5% error), a series of meshes were tested under the same solution setup conditions for each in order to examine the effect of different mesh parameters on the simulated pressure drop. The resulting pressure drops for the test meshes can be seen in Table 6 below:

Element Size	Boundary Layers?	BL Total Thickness (m)	Number of BL	ΔP in 10cm (Pa)	ΔP/L in 1m (Pa/m)
$D_p/20$	No	n/a	n/a	217.9	2179
$D_p/20$	Yes	0.00032	5	258.2	2582
$D_p/30$	Yes	0.0001	10	90.2	902
$D_p/40$	No	n/a	5	223.8	2238
$D_p/40$	Yes	0.00032	5	298.3	2983
$D_p/40$	Yes	0.00016	10	292.5	2925
$D_p/40$	Yes	0.0001*	10	84.7	847

Table 6: Single phase pressure drop in the 10cm empty channel for various meshes (*first layer thickness of 0.00001m was specified for this mesh for total thickness of 0.0001m)

As the table shows, none of the tests ever approached the expected 1001 Pa/m pressure drop within a reasonable margin of error. Upon revisiting the calculation, it was determined that the relationship between the Moody friction factor and the Reynolds number was actually not best represented by the proportionality constant of 64 as is common for most open channels. In fact, due to the square geometry of the channel, the proportionality constant was determined to actually be closer to approximately 56.91, which resulted in an expected pressure drop of approximately 891 Pa/m (White, 1991). This corrected pressure drop was ultimately deemed more acceptable than the originally calculated 1001 Pa/m. Based on this new value, the pressure drop for the final mesh exhibited a percent error of 1.2%.

4.2.2 Single Phase Flow: Packed Channel

Single phase flow in a packed channel was examined in order to prove that simulations could be completed when packing in the channel was included. Similar to the simulations for a single phase in the empty channel, the pressure drop across a packed channel was compared to a calculated pressure drop in order to assess the program's computing capabilities around packing particles. The 40- and 36-sphere models were used for this set of simulations. These models were chosen because they would not take as much time to iterate a solution; however they were also sufficiently long enough to fully develop the flow in the channel since common CFD practice has shown that fully developed flow occurs after a few particles when there is packing in a channel. The fluid for these simulations was air at 0.5 m/s, which closely approximated gaseous nitrogen, and the mesh was the same as had been developed for the empty channel. A calculated pressure drop was found according to the Ergun equation:

$$\frac{\Delta P}{L} = \frac{150 V_{air} \mu_{air}}{\Phi_s^2 D_p^2} * \frac{(1-\varepsilon)^2}{\varepsilon^3} + \frac{1.75 \rho_{air} V_{air}^2}{\Phi_s D_p} * \frac{1-\varepsilon}{\varepsilon^3}$$

In this equation, V is the velocity, μ is the viscosity, ϕ_s is the particle sphericity (which is one for spherical particles), D_p is the packing particle diameter, ε is the void fraction, and ρ is the density. The pressure drop obtained from this calculation was approximately 248 Pa/m.

The pressure drops that were obtained from the FLUENT simulations can be seen in Table 7 below:

Model	Pressure Drop (Pa/m)
Diagonally-packed 40 sphere section	408
Bottom-packed 36 sphere section	309
Spiral-packed 36 sphere section	670

Table 7: Pressure drop from FLUENT for air in a packed channel

While these pressure drops are on the same order of magnitude as the anticipated (calculated) pressure drop, all three results are over-predictions in comparison to the Ergun result. One possible reason for the discrepancy was discussed in a report titled "CFD modelling and experimental validation of pressure drop and flow profile in a novel structured catalytic reactor packing" by Calis et al. (2001). In this report, the researchers examined single phase pressure drop in channels with very few particles to assess the validity of the Ergun equation. Calis et al. (2001) even examined a channel with a square cross-section and spherical particles placed in a diagonal packing pattern exactly like the diagonally-packed model that was developed for this project. The major result that Calis et al. (2001) reported was that while CFD and laboratory experiments agreed on single phase pressure drop in a packed channel within a 10% error of one another, Ergun was reported to over-predict the friction factor (and therefore pressure drop) by approximately 80% (Calis et al., 2001). This very large discrepancy between Ergun and CFD results seems to support that the simulated pressure drops seen above are not within a small range of error from the calculated pressure drop.

Other factors that may have created discrepancies between the calculated and simulated pressure drops include the fact that the Ergun equation was developed based on cylindrical, not square, channels, and this may have resulted in an incorrect calculated pressure drop. Also, there were some anomalies observed in the FLUENT-simulated velocity profiles at the channel outlet and also in the spaces between particles and the channel wall (around the bridges). These phenomena can be observed in Figure 26 through Figure 31 below for the diagonally-packed, bottom-packed, and spiral-packed channels:

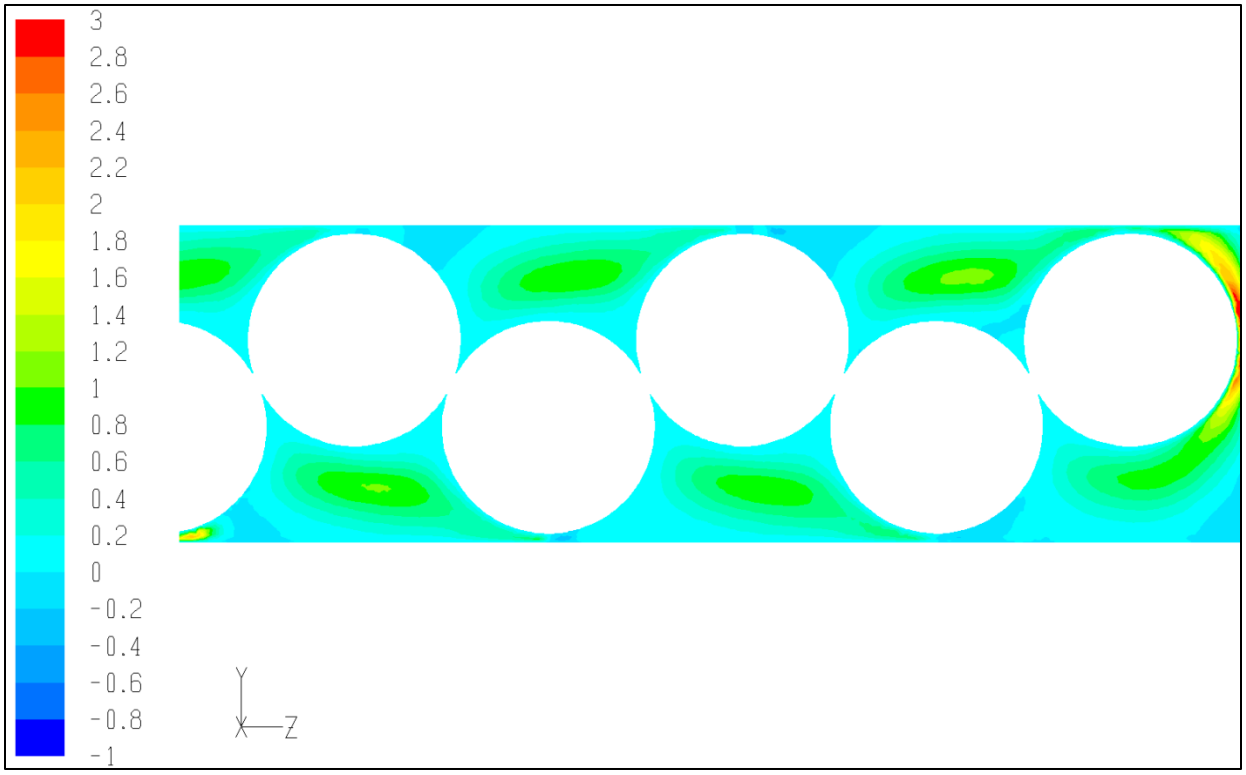

Figure 26: Diagonally-packed outlet velocity profile for single phase (velocity in m/s)

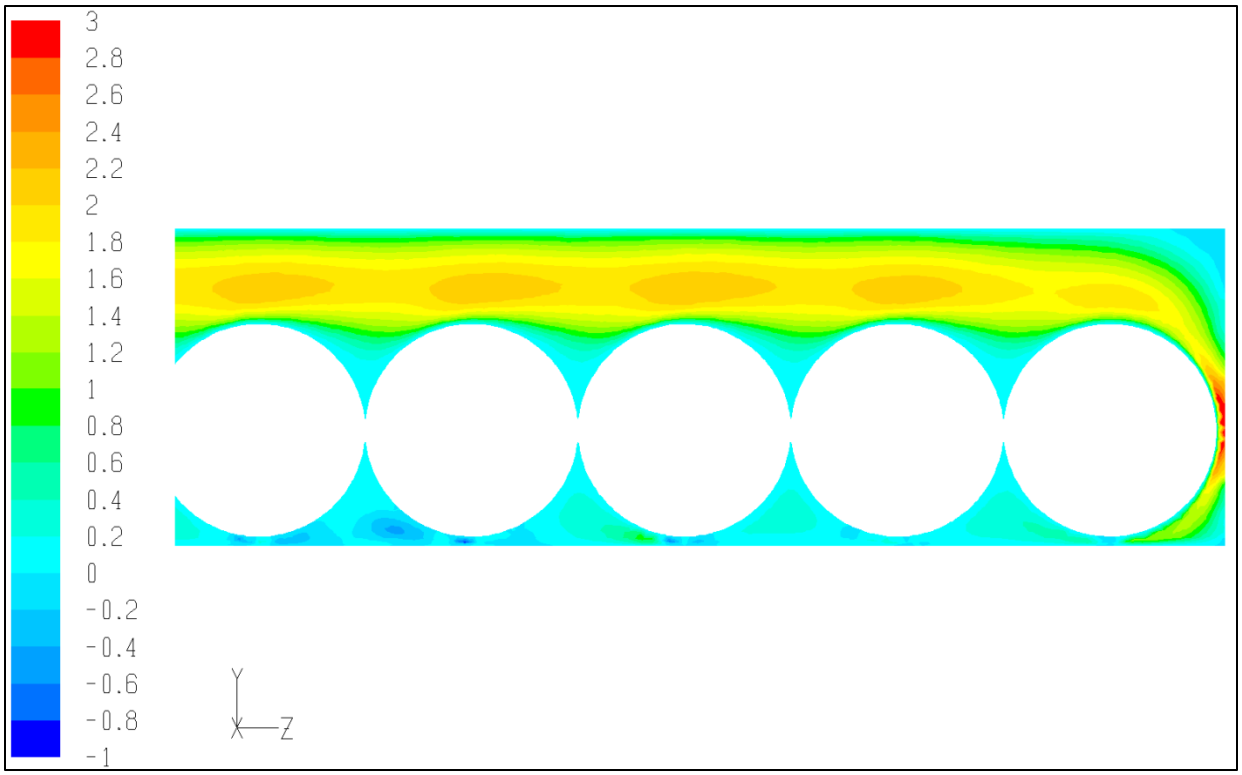

Figure 27: Bottom-packed outlet velocity profile for single phase (velocity in m/s)

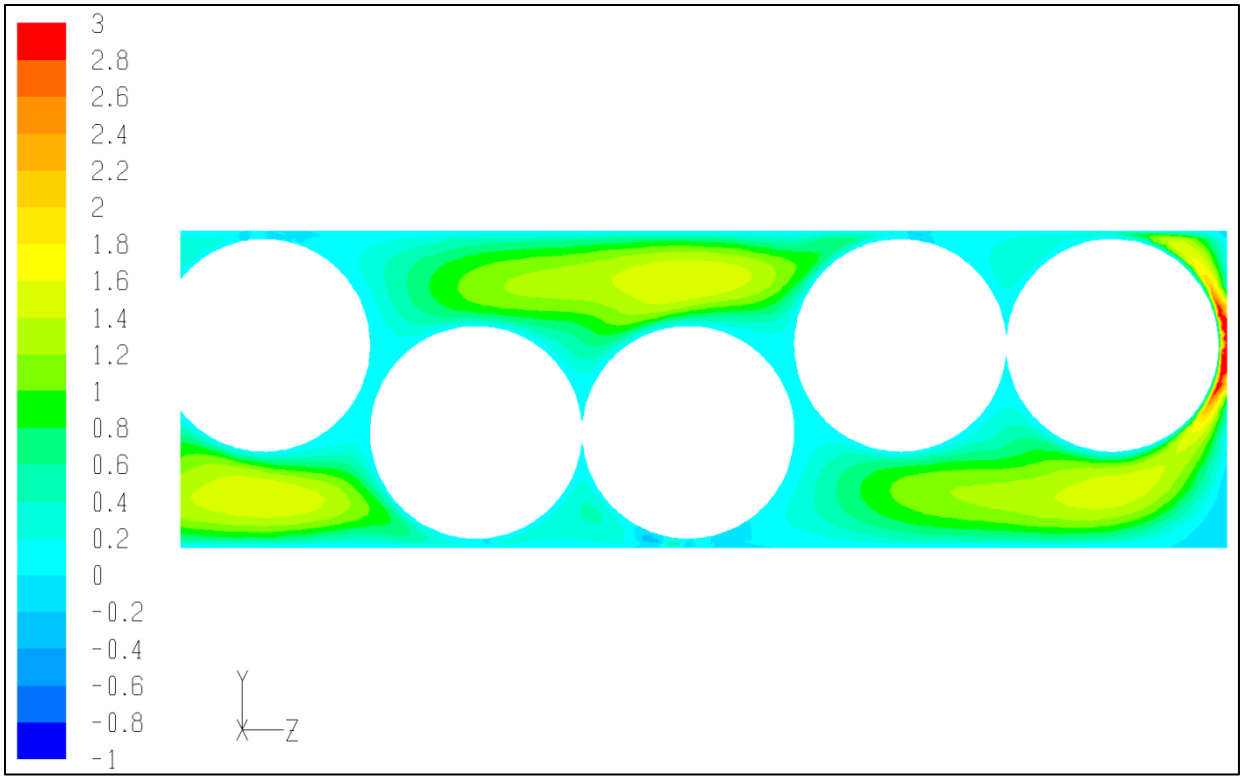

Figure 28: Spiral-packed outlet velocity profile for single phase (velocity in m/s)

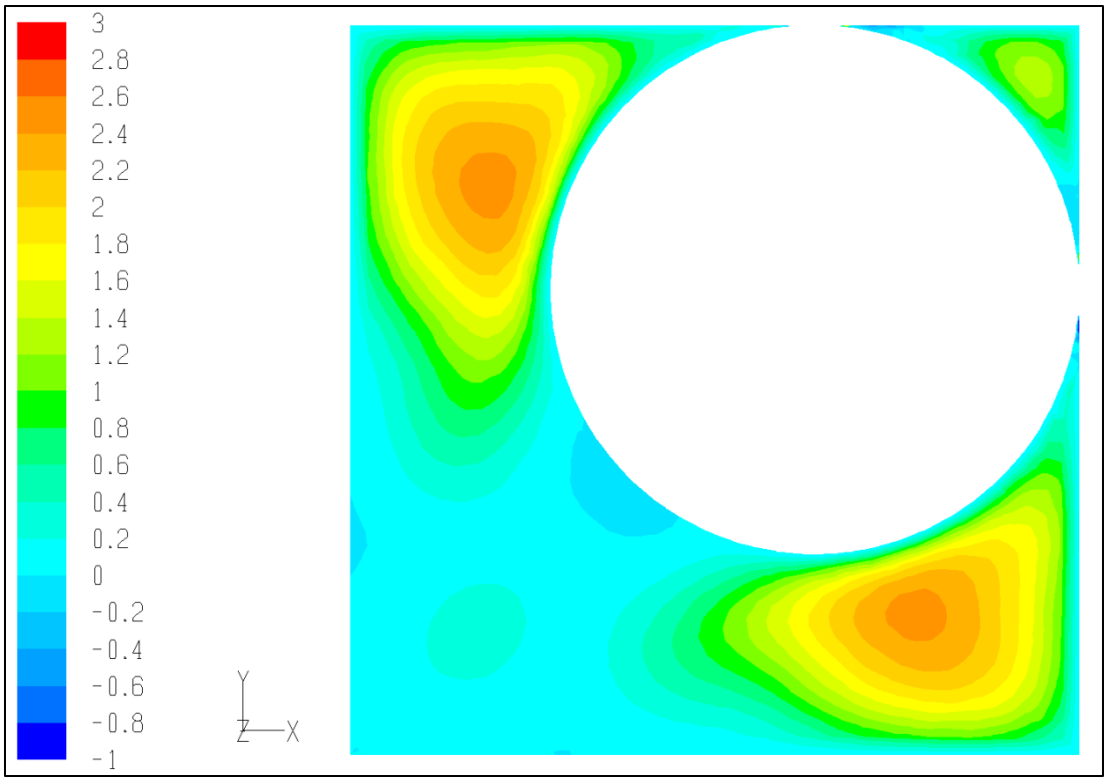

Figure 29: Diagonally-packed single phase velocity profile at sphere-wall bridge (velocity in m/s)

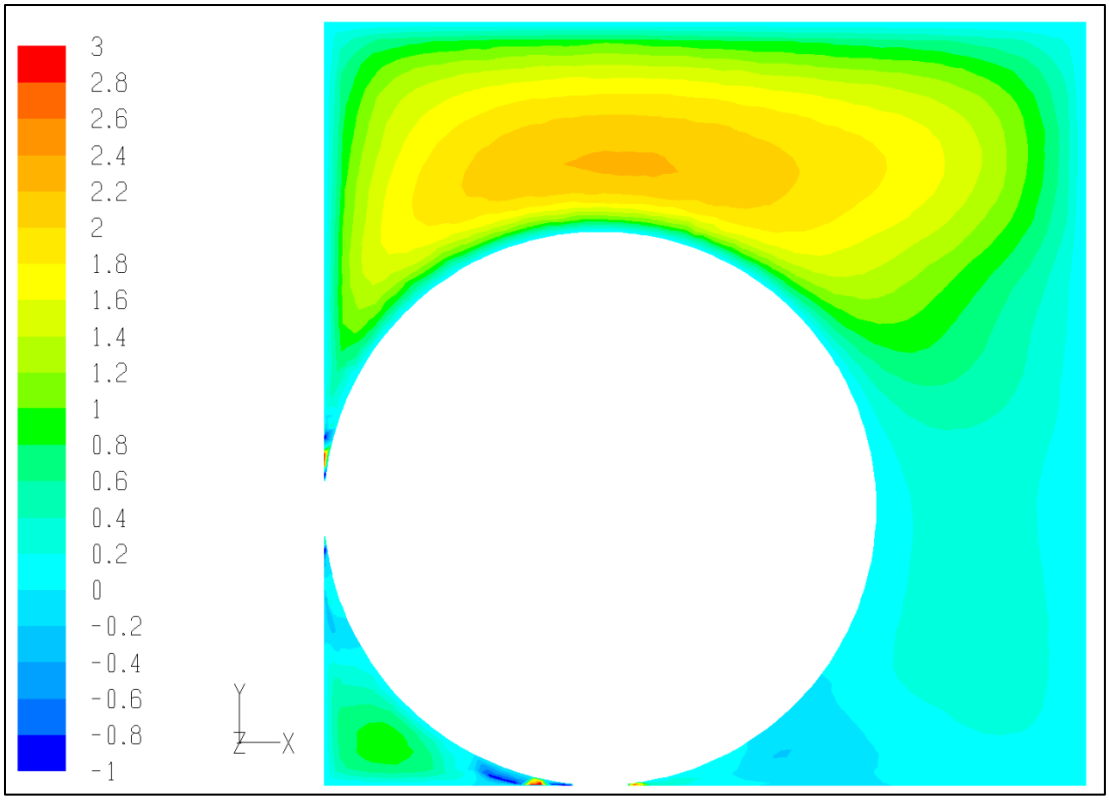

Figure 30: Bottom-packed single phase velocity profile at sphere-wall bridge (velocity in m/s)

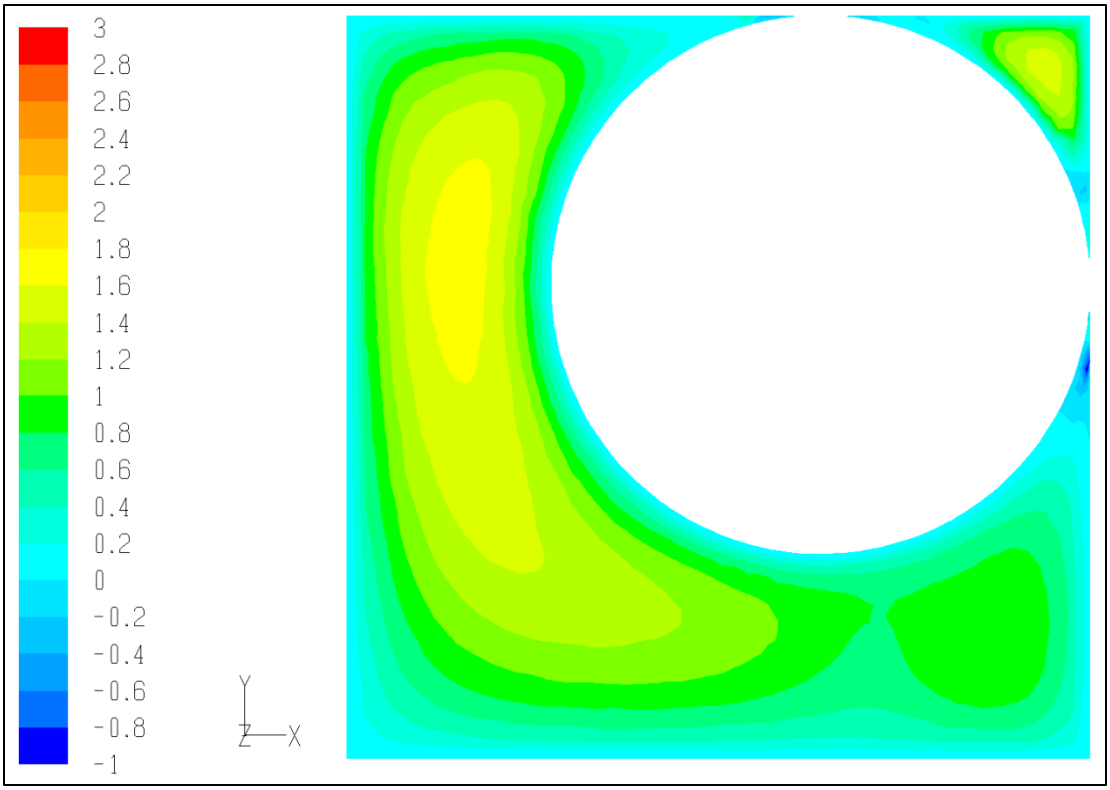

Figure 31: Spiral-packed single phase velocity profile for sphere-wall bridge (velocity in m/s)

The red zones in the figures depicting channel outlets show that the velocities were supposedly increasing quite a bit as the air exited the channel, which does not seem in accordance with the consistent green and yellow colors observed in the rest of the velocity profile. These red zones are most likely evidence of the need for an exit length at the end of the channel to avoid backmixing, which probably caused the velocity abnormalities. The deep red zones observed near the sphere-wall bridges indicate that the velocities were calculated as being incredibly high in these regions, which does not make much physical sense since the velocity should be close to zero at the walls due to the no-slip boundary conditions. This anomaly is indicative of issues with the mesh, and particularly the boundary layers, in the small spaces between particles and the walls. It is likely that when the boundary layer cells were created around the sphere-wall bridges, they had to either be compressed or stepped down in order to fit the cells into such a small space; this mesh tactic can cause problems with iterations for these cells since they are so small in comparison to the surrounding cells. These phenomena, as suggested before, may have had something to do with the inaccuracy of the pressure drop results obtained from FLUENT when compared to the pressure drop results obtained from the Ergun equation.

4.2.3 Multiphase Flow: Empty Channel

Multiphase flow in an empty channel was examined in order to determine program capabilities with multiple phases. For this case only the 10cm empty channel was used in two-dimensions (height and length) to decrease the mesh size and also the amount of time spent on iterations since incorporating an additional phase in the simulation was taxing on the program's computing capabilities. Liquid water and nitrogen were given velocities of 0.5 m/s and 10 m/s, respectively. Similar to the single

phase empty and packed channel trials, a calculated pressure drop was determined in order to compare against simulated pressure drop results to assess the accuracy of FLUENT. A series of equations that are part of the Lockhart-Martinelli method were used to calculate an approximate anticipated multiphase pressure drop of 22,236 Pa/m.

Both the mixture (i.e. algebraic-slip) and Eulerian models were tested in FLUENT with little success. The simulated pressure drop results can be seen in Table 8 below:

Model/# of Iterations	Static Inlet Pressure (Pa)	Pressure Drop (Pa/m)
Mixture, 400 iterations	1,050	52,490
Mixture, 250 iterations	1,228	61,414
Eulerian, 500 iterations	1,009	50,456
Eulerian, 750 iterations	956	47,799
Eulerian, 1000 iterations	963	48,160
Eulerian, 1250 iterations	959	47,970

Table 8: Simulated multiphase empty channel pressure drops using mixture and Eulerian models

The mixture model was originally used to simplify the calculations for the program, however within the 400 iterations performed with the mixture model, the residuals for the mixture model started to become unsteady around the 250th iteration. The iterations were then restarted using the mixture model for the first 250 iterations and then switching to the Eulerian model for the remaining iterations. Despite this, the pressure drops obtained from FLUENT were more than twice the anticipated pressure drop found using the Lockhart-Martinelli method. After observing this, the fluid velocities were changed to those of the article by Vonortas et al. (2010) (water at $5x10^{-5}$ m/s and nitrogen at $1x10^{-3}$ m/s) to see how the solution would change given much lower fluid speeds. In this case, the solution immediately diverged and was deemed unworthy of further investigation.

After the failure of both the mixture and Eulerian models for the chosen fluid velocities, the volume fraction profiles for the channel were examined and it was discovered that the fluids were actually in stratified flow, unlike the original assumption of bubbly or plug flow. This fluid stratification at the channel inlet can be seen in Figure 32 below:

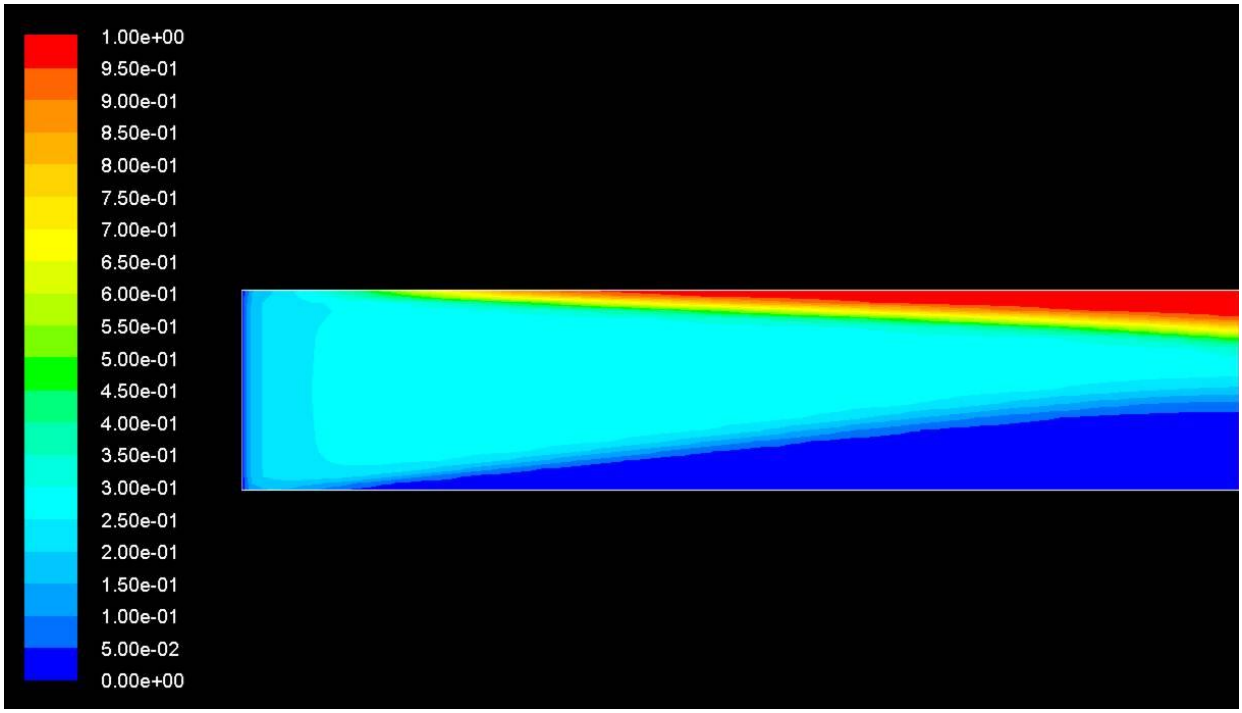

Figure 32: Volume fraction profile of nitrogen in 10cm empty channel

In the figure, dark blue represents 100% water and deep red represents 100% nitrogen, so the phases can be observed to be separating at the beginning of the channel. The stratification observed between the fluids matched the observations of Vonortas et al. (2010) that most of the liquid was at the bottom of the channel. The stratification also suggested that this project may have actually required a volume of fluid (VOF) model in order to be able to simulate the multiphase conditions of Vonortas et al. (2010) because the VOF model is applicable to stratified flow whereas the mixture and Eulerian models are not. Unfortunately, the VOF model was outside of the scope of this project so it was not pursued any further.

The 10cm empty channel was used to test multiphase flow in one other simulation to observe how the mixture and Eulerian models fared with higher fluid velocities. Water and nitrogen were given velocities of 45 m/s and 35 m/s, respectively, in accordance with a CFD study that had tested all multiphase flow regimes present in the Baker chart to prove that CFD programs are capable of solving all flow regimes given specific flow conditions (De Schepper et al., 2008). The volume fraction and pressure profiles for the multiphase simulation in an empty channel at high fluid velocities can be seen in Figure 33 and Figure 34 below:

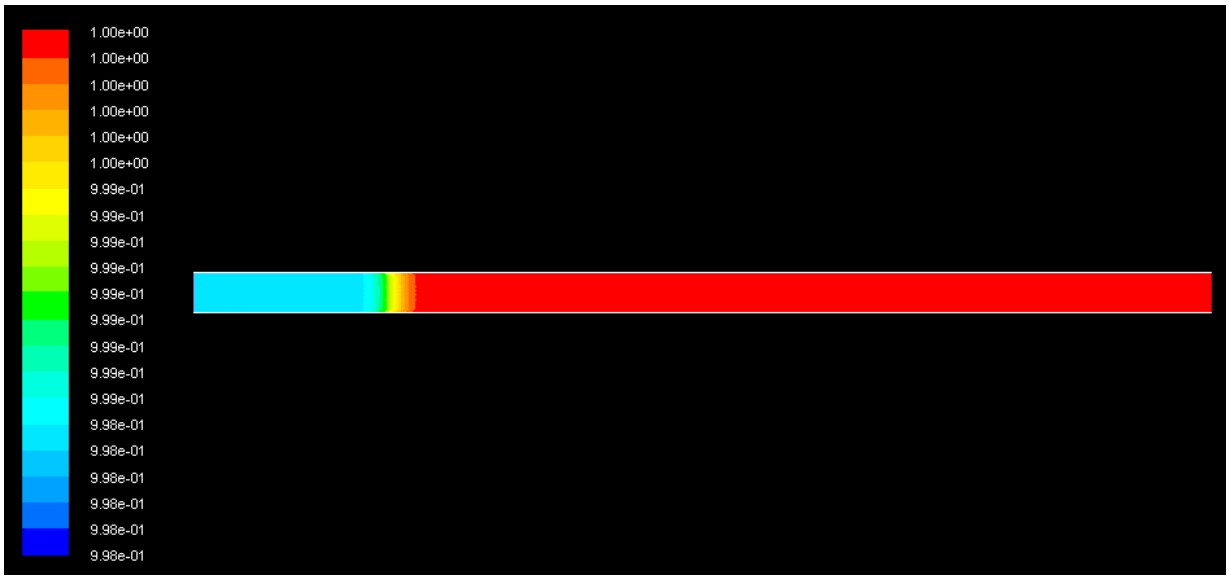

Figure 33: Volume fraction profile of water in 10cm empty channel, 800 iterations

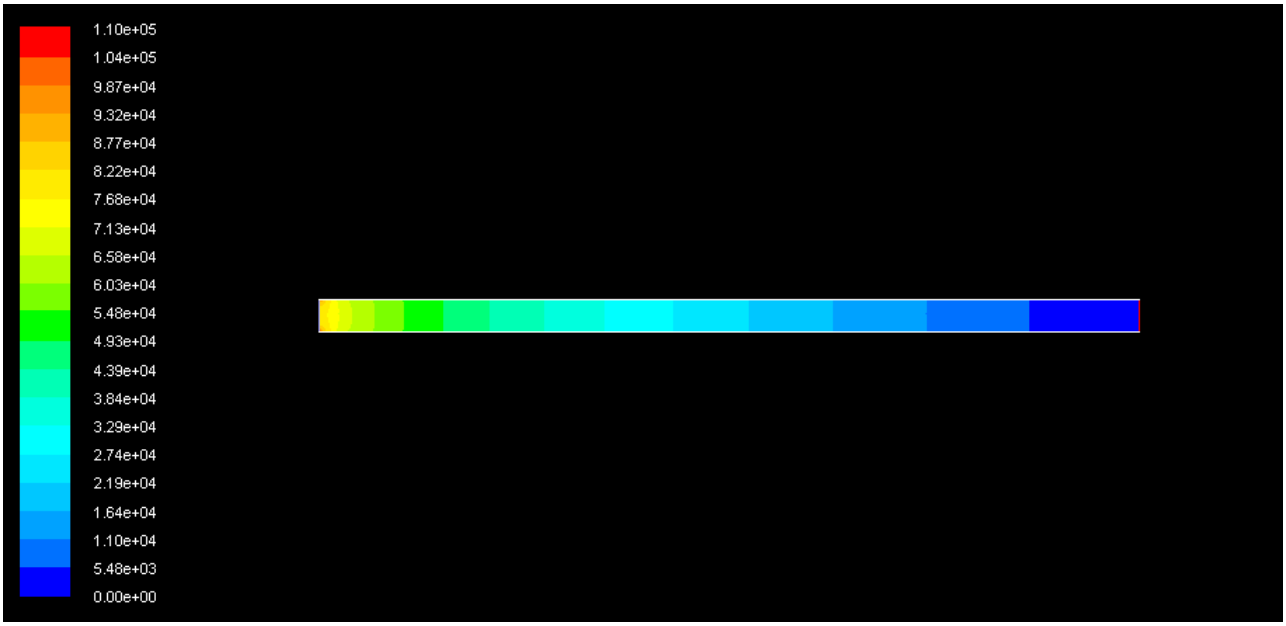

Figure 34: Pressure profile of multiphase flow in 10cm empty channel

As the figures show, the higher fluid velocities resulted in a pressure profile that made physical sense; however the volume fraction profile was not physically accurate. In the pressure profile, the change from red to blue from inlet to outlet shows that the pressure is highest at the inlet and lowest at the outlet, as would be expected in real life. The volume fraction profile is not as comparable to real life. The sharp contrast between the teal blue towards the inlet and the red towards the outlet indicates that the program calculated most of the nitrogen to be backed up towards the inlet (nitrogen is represented by blue) and most of the water was concentrated towards the outlet (water is represented by red). This

does not match the description of bubbly flow, where the blue and red should have appeared interspersed throughout the channel.

Further iterations showed an interesting phenomenon in the volume fraction profile. Added iterations resulted in a shift in the volume fraction profile, shown in Figure 35 below:

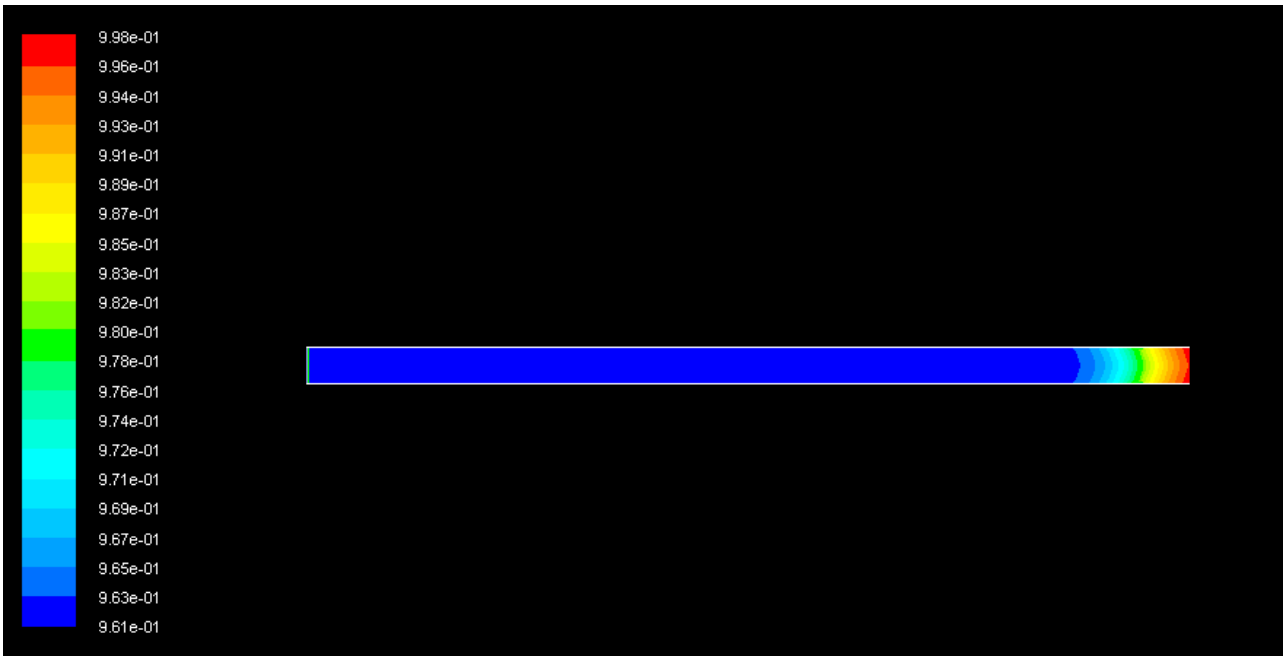

Figure 35: Volume fraction profile of water in 10cm empty channel, 4000 iterations

The shift in the volume fraction profile shows that the program calculated water (represented as red) as being more highly concentrated towards the outlet whereas nitrogen (represented as blue) was more highly concentrated throughout the majority of the channel. Further iterations showed a complete shift of higher nitrogen concentrations taking over the entire channel length with virtually no high water concentrations represented. This may be indicative of the program using a time-stepping method on a steady state calculation, which could be the source of error when attempting to simulate a bubbly flow. Another issue may have been that the mixture and Eulerian models are intended for problems in which the secondary phase is dilute and is also the fluid with the lesser density. The specifications for the project actually had nitrogen in excess with water as being dilute in the nitrogen, suggesting that nitrogen was the primary phase. Since this was not going to be compatible with the solver, the primary phase was set as water with nitrogen as being dilute; however the fluid velocities remained the same and therefore may have contributed even more to the inaccuracies. It was also noted that alterations to the volume fraction resulted in an incorrect mass balance, where the amount of fluid entering the channel was not the same as the amount of fluid exiting the channel. In particular, increasing the volume fraction and velocity of the secondary phase (nitrogen) skewed the mass balance to an even greater degree, which is most likely a result of the limitations of the solver.

4.2.4 Multiphase Flow: Packed Channel

The final set of simulations was conducted with multiphase flow in a packed channel as was specified in the project problem statement and project goals. The 4-sphere models were used to keep solution iteration time at a minimum. Liquid water and nitrogen were tested at all 3 sets of fluid velocities to examine how well the mixture and Eulerian models could solve the geometric models. These solutions included both the project conditions of low flows in the laminar regime and also additional multiphase conditions of high flows that would be more likely to work with the mixture and Eulerian models. The first simulation with water at $5x10^{-5}$ m/s and nitrogen at $1x10^{-3}$ m/s was unsuccessful per expectations of stratified flow from the empty channel discussed above. From here, velocities were increased to 0.5 m/s for water and 10 m/s for nitrogen and the solution process was repeated using the mixture and Eulerian models. Due to an issue with FLUENT, a volume fraction profile visual could not be obtained; however the volume fractions of water at several points along the channel length were recorded and plotted to observe the trend. The volume fraction of water along the 4-sphere diagonally-packed channel can be seen in Figure 36 below:

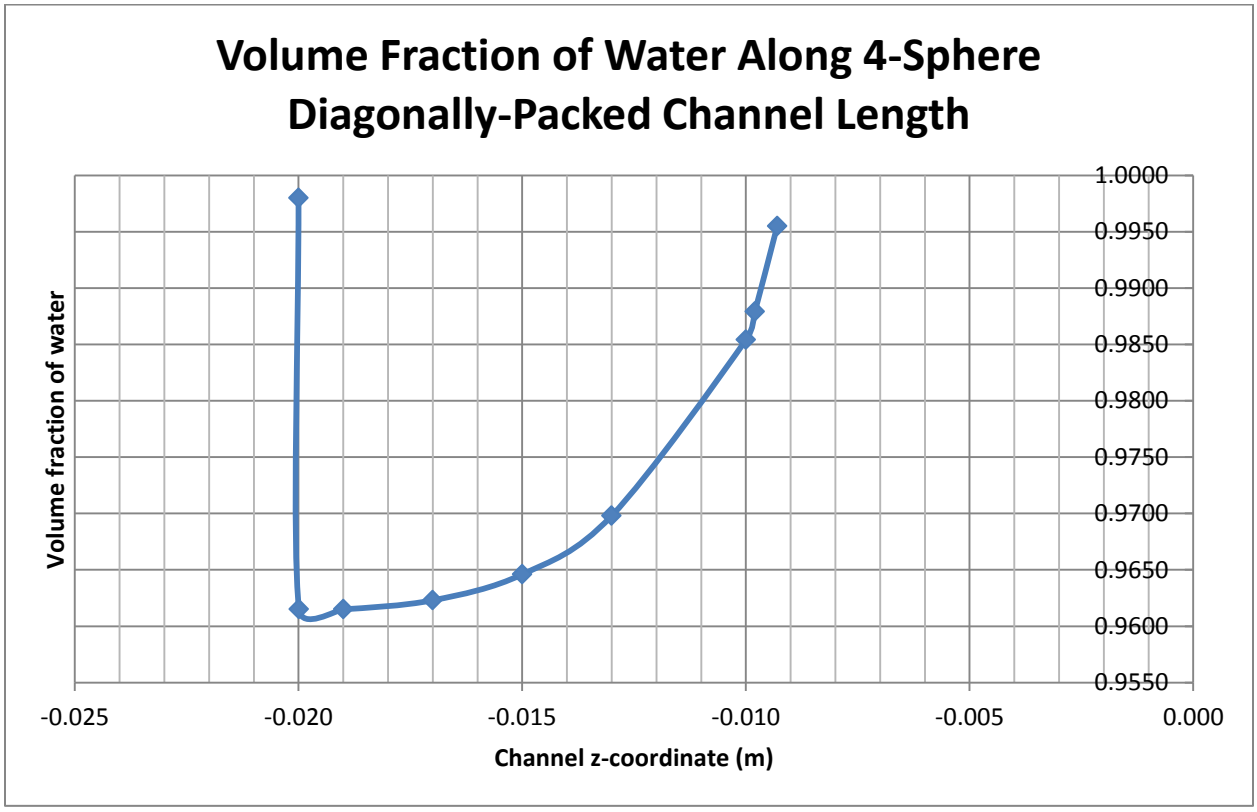

Figure 36: Volume fraction of water in 4-sphere diagonally-packed channel

The graph shows that FLUENT originally calculated the volume fraction of water to be the specified volume fraction of 0.998 but immediately decreased the volume fraction to adjust for other calculations. The volume fraction of water is then seen to steadily increase towards the outlet of the channel back to the original volume fraction. Unfortunately, without a visual volume fraction profile, it was difficult to conclude whether the flow was stratified similar to the stratified result from the 10cm empty channel or

if the flow was being calculated in a time-stepping fashion similar to the high velocity result in the 10cm empty channel.

Finally, water and nitrogen were set to 45 m/s and 35 m/s, respectively, in order to observe if the mixture and Eulerian models would iterate a solution for multiphase flow in a packed channel with velocities in the bubbly flow regime. After many alterations to secondary phase conditions (i.e. granular condition or no granular condition), turbulence conditions (under the viscous model), specified operating density, volume fraction of the secondary phase, and turbulent kinetic energy (under velocity inlet), the mixture and Eulerian solvers repeatedly diverged after 2-5 iterations. The divergence may be a result of the program's lack of capabilities to handle multiple phases with packing in a turbulent multiphase model that showed inconsistencies even for the 10cm empty channel.

Chapter 5: Conclusions and Recommendations

A number of important conclusions regarding CFD program capabilities and simulations of multiphase flow could be drawn from this project. First, ANSYS 13.0 was determined to be a user-friendly CFD software package, however it was difficult to develop program expertise which led to a variety of issues throughout the course of this project. On the other hand, GAMBIT and FLUENT were determined to have a much higher learning curve but presented significantly fewer issues in the long run. This leads to the first project recommendation that GAMBIT and FLUENT, rather than ANSYS, be used for highly specific and complicated research projects because of the greater amount of user-control that exists in these programs.

The second major conclusion was that the specified combination of multiphase flow rates and CFD solver were not compatible with one another since the mixture and Eulerian solvers are more suited to flows at higher rates. Due to this disconnect between the flow parameters specified and the solvers, only flow regime and pressure drop could be thoroughly explored during this project. In terms of these comparison parameters specified in the project goals, the flow regimes and pressure drops were found to be predicted accurately for some cases in which careful consideration for the flow specifications and solver type was able to be fully explored to ensure proper execution. Further research would be required in order to obtain higher accuracy for multiphase flow in packed channels and to examine comparisons between liquid holdup and axial dispersion. This leads to the second project recommendation that future studies involving a similar type of setup be conducted using a volume of fluid model or the CFX solver available in ANSYS (if ANSYS were to be chosen). Literature research conducted throughout this project suggested that the VOF model or CFX solver might have produced a higher level of success with the flow rates specified for this project, so these may be options worth investigating in the future.

Works Cited

(2011). Retrieved from CFD Online: http://www.cfd-online.com/

Calculating Two-Phase Pressure Drop with the Lockhart-Martinelli Method. (2011, May). Retrieved from Excel Calculations: Free Chemical and Petroleum Engineering Spreadsheets: http://excelcalculations.blogspot.com/2011/05/calculating-two-phase-pressure-drop.html

Andersson, B., Andersson, R., Hakansson, L., Mortensen, M., Sudiyo, R., & van Wachem, B. (2012). Chapter 6: Multiphase Flow Modeling. In B. Andersson, R. Andersson, L. Hakansson, M. Mortensen, R. Sudiyo, & B. van Wachem, *Computational Fluid Dynamics for Engineers* (pp. 143-173). New York: Cambridge University Press.

ANSYS, Inc. (2010, November). ANSYS Workbench User's Guide. Canonsburg, Pennsylvania, United States of America.

Bakker, A. (2008, February 3). *Computational Fluid Dynamics Lectures: Lecture 14. Multiphase flow.* Retrieved from The Colorful Fluid Mixing Gallery: http://www.bakker.org/dartmouth06/engs150/

Bakker, A., Haidari, A., & Oshinowo, L. M. (2001). Realize Greater Benefits from CFD. *Chemical Engineering Progress*, 45-54.

Calis, H., Nijenhuis, J., Paikert, B., Dautzenberg, F., & van den Bleek, C. (2001). CFD modelling and experimental validation of pressure drop and flow profile in a novel structured catalytic reactor packing. *Chemical Engineering Science*, 1713-1720.

De Schepper, S., Heynderickx, G., & Marin, G. (2008). CFD modeling of all gas-liquid and vapor-liquid flow regimes predicted by the Baker chart. *Chemical Engineering Journal*, 349-357.

Denn, M. M., & Russell, T. (1980). Chapter 18: Two-Phase Gas-Liquid Flow. In M. M. Denn, *Process Fluid Mechanics* (pp. 342-355). Englewood Cliffs: Prentice-Hall Inc.

Fluent Inc. (2006). FLUENT 6.3 User's Guide. Lebanon, New Hampshire, United States of America.

Fox, R. W., Pritchard, P. J., & McDonald, A. T. (2009). *Introduction to Fluid Mechanics (7th Edition).* United States of America: John Wiley & Sons, Inc.

Gunjal, P., Kashid, M., Ranade, V., & Chaudhari, R. (2005, February 23). Hydrodynamics of Trickle-Bed Reactors: Experiments and CFD Modeling. *Industrial and Engineering Chemistry Research*, pp. 6278-6294.

Lopes, R. J., & Quinta-Ferreira, R. M. (2009, January 27). Numerical Simulation of Trickle Bed Reactor Hydrodynamics with RANS-Based Models Using a Volume of Fluid Technique. *Industrial and Engineering Chemistry Research*, pp. 1740-1748.

McCabe, W., Smith, J., & Harriott, P. (2005). Chapter 7: Flow Past Immersed Objects. In W. McCabe, J. Smith, & P. Harriott, *Unit Operations of Chemical Engineering (7th Edition)* (pp. 155-193). New York: McGraw-Hill.

Mills, P., Ramachandran, P., & Chaudhari, R. (1992). Multiphase Reaction Engineering for Fine Chemicals and Pharmaceuticals. *Reviews in Chemical Engineering*, pp. 45-56; 142-151.

Vonortas, A., Hipolito, A., Rolland, M., Boyer, C., & Papayannakos, N. (2010). Fluid Flow Characteristics of String Reactors Packed with Spherical Particles. *Chemical Engineering Technology*, 208-216.

White, F. M. (1991). *Viscous Fluid Flow: Second Edition.* United States of America: McGraw-Hill, Inc.

Appendix

Appendix A: Calculated Sphere Origins and Creating Bridge Geometries

A.1 Calculating Sphere Origins for Various Models

In order to calculate how many spheres could fit into the meter long duct, the origins of the spherical particles for the three different models were calculated. This was calculated using excel and basic geometry concepts.

Diagonally-Packed Model

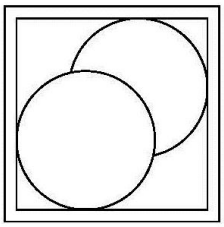

Figure A.1.1: Front View drawing of diagonally-packed channel (XY axis)

The diagonally-packed tube has distinct symmetry in that spheres are stacked directly in front of the sphere two before it on the z-axis. If the bottom left corner on the inside of the tube was considered to be the origin, O(0mm, 0mm, 0mm) and the top right the corner R(4mm, 4mm, 0mm), the center of the first sphere is located at S1(1.45mm, 1.45mm, z1) and the second sphere is located at S2(2.55mm, 2.55mm, z2). The distance between centers of spheres in the z-direction was calculated using the three dimensional Pythagorean theorem:

$$2r = d = \sqrt{(x_2 - x_1)^2 + (y_2 - y_1)^2 + (z_2 - z_1)^2}$$

Where $(x_2 - x_1) = (y_2 - y_1) = 1.1mm$ by symmetry on the xy axis, r represents radius and d represents diameter($d = 2.9mm$).

Rearranging this equation yields:

$$(z_2 - z_1) = \sqrt{(2.9mm)^2 - 2(1.1mm)^2}$$

Due to symmetry, the distance in the z-direction between each sphere origin can be determined by the above equation. Using this equation, the amount of spheres in a fully packed diagonally-packed tube in one meter or less is 408 spheres.

Bottom-Packed Model

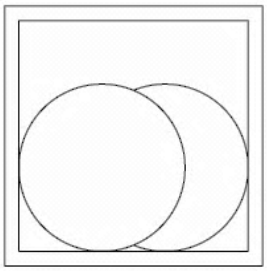

Figure A.1.2: Front View drawing of bottom-packed channel (XY axis)

Particles in the bottom-packed model, like particles in the diagonally packed model, have the same x and y coordinates as the particle two spheres ahead of it. If the bottom left corner on the inside of the tube was considered to be the origin, O(0mm, 0mm, 0mm) and the top right the corner R(4mm, 4mm, 0mm), the center of the first sphere is located at S1(1.45mm, 1.45mm, z1) and the second sphere is located at S2(2.55mm, 1.45mm, z2). In this case, the same methodology was applied to find the distance in the z-direction between particle origins. The Pythagorean theorem was applied:

$$2r = d = \sqrt{(x_2 - x_1)^2 + (y_2 - y_1)^2 + (z_2 - z_1)^2}$$

Where $(x_2 - x_1) = 1.1mm$ and $(y_2 - y_1) = 0$, r represents radius and d represents diameter($d = 2.9mm$).

Rearranging this equation yields:

$$(z_2 - z_1) = \sqrt{(2.9mm)^2 - (1.1mm)^2}$$

Using this equation, the amount of spheres in a fully packed bottom-packed tube in one meter or less is 372 spheres.

Spiral-Packed Model

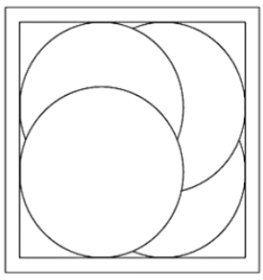

Figure A.1.3: Front View drawing of spiral-packed channel (XY axis)

The spiral packed model displayed a repeating pattern of 4 spheres, with coordinates of S1(1.45mm, 1.45mm, z1), S2(1.45mm, 2.55mm, z2), S3(2.55mm, 2.55mm, z3), and S4(2.55mm, 1.45mm, z4). Again, the Pythagorean theorem was applied:

$$d = \sqrt{(x_2 - x_1)^2 + (y_2 - y_1)^2 + (z_2 - z_1)^2}$$

Where either $(x_2 - x_1) = 1.1mm$ and $(y_2 - y_1) = 0mm$, or $(x_2 - x_1) = 0mm$ and $(y_2 - y_1) = 1.1mm$. In either case, rearranging this equation yields the same equation as the bottom packed channel:

$$(z_2 - z_1) = \sqrt{(2.9mm)^2 - (1.1mm)^2}$$

Using this equation, the amount of spheres in a fully packed spiral-packed tube in one meter or less is 372 spheres.

Particle Origins:

Diagonally Packed			
Sphere-n	**x-coord**	**y-coord**	**z-coord**
408	2.55	2.55	997.56
1	1.45	1.45	1.45
2	2.55	2.55	3.90
3	1.45	1.45	6.34
4	2.55	2.55	8.79
5	1.45	1.45	11.24
6	2.55	2.55	13.69
40	2.55	2.55	96.90
408	2.55	2.55	997.56
409	1.45	1.45	1000.01

Bottom Packed			
Sphere-n	**x-coord**	**y-coord**	**z-coord**
372	2.55	1.45	996.95
1	1.45	1.45	1.45
2	2.55	1.45	4.13
3	1.45	1.45	6.82
4	2.55	1.45	9.50
5	1.45	1.45	12.18
6	2.55	1.45	14.87
36	2.55	1.45	95.36
372	2.55	1.45	996.95
373	1.45	1.45	999.63

Spiral Packed			
Sphere-n	x-coord	y-coord	z-coord
372	2.55	1.45	996.95
1	1.45	1.45	1.45
2	1.45	2.55	4.13
3	2.55	2.55	6.82
4	2.55	1.45	9.50
5	1.45	1.45	12.18
6	1.45	2.55	14.87
36	2.55	1.45	95.36
372	2.55	1.45	996.95
373	1.45	1.45	999.63

A.2 Creating Geometry in SolidWorks

A particle has four contact points; two on the wall and two with the adjacent spheres. When building the geometry in SolidWorks, a sphere was drawn with a coordinate system at the origin of the sphere. Cylindrical bridges were built at all contact points between particles and other particles or the wall at a diameter size of 2.9e-04 m, a tenth of the particle diameter.

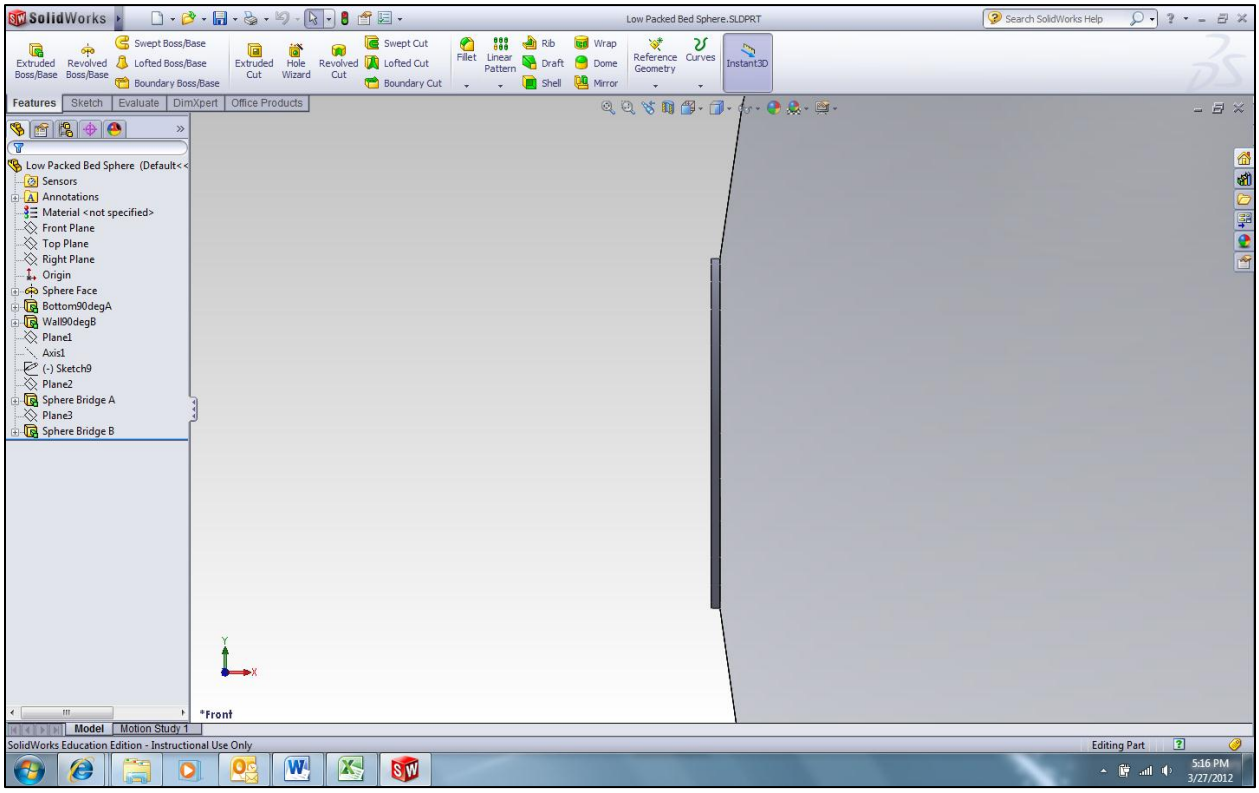

Figure A.2.1: Contact point bridge

Shown in the figure above, the bridge extends no further than the contact point on the sphere. Each bridge was created on a plane that divided the origin and extruded perpendicularly 1.45e-03 m to create a bridge. Planes for contact points with the wall were drawn on the planes in the SolidWorks coordinate system. Planes for bridges at the contact points between particles were created by locating where the contact points were, drawing an axis from the contact point to the sphere origin and creating a plane perpendicular to the axis and was also coincident with the origin of the sphere.

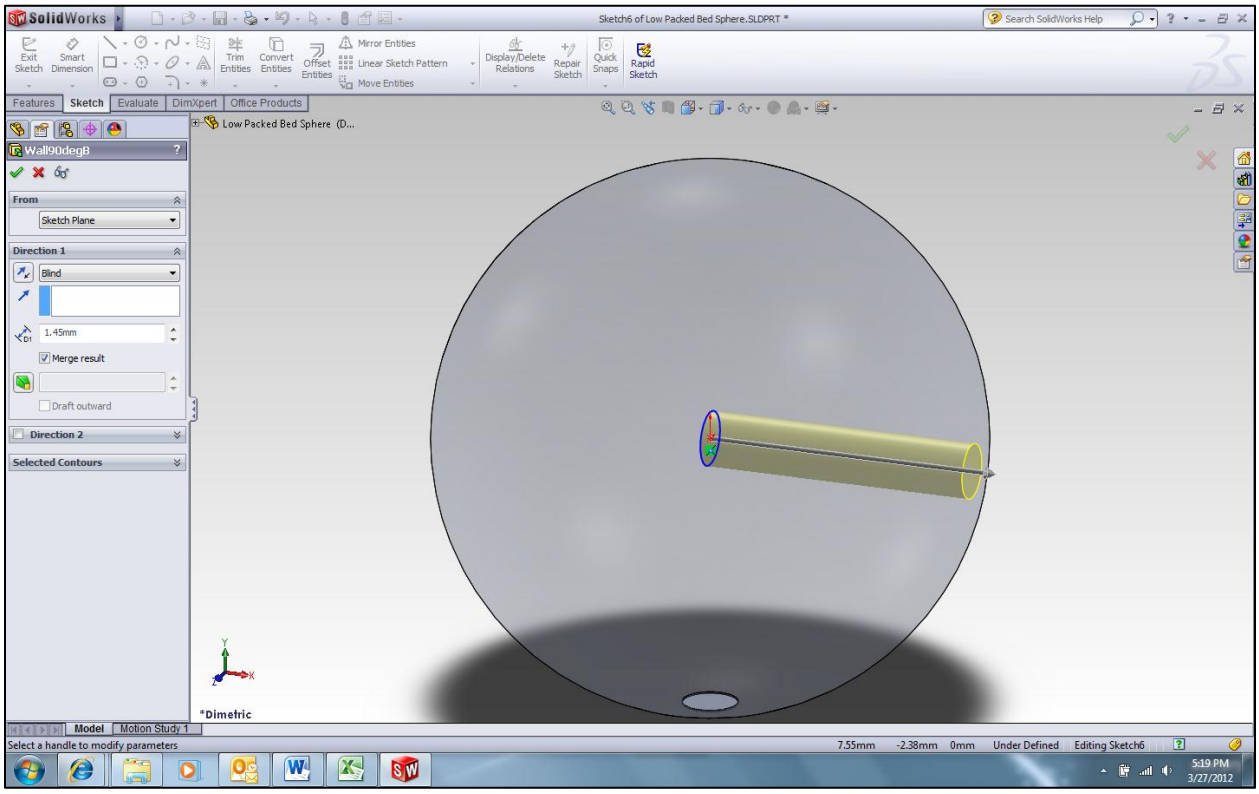

Figure A.2.2: Contact point bridge extrusion

After spheres with bridges were created, the sphere was then used in an assembly to create a packed channel. Two contact point bridges were mated to create a bridge between spheres. After the assembly, the combine>join feature was used to make a solid part. It was then saved as an ACIS file to import into ANSYS to fill and mesh the geometry.

Diagonally-Packed Model Sphere:

To make the bridges on the diagonally packed-sphere, the bridge to the bottom of the channel was drawn on the zx-plane and extruded in the negative z direction. The bridge to the wall was drawn on the yz-plane and extruded in the positive x direction.

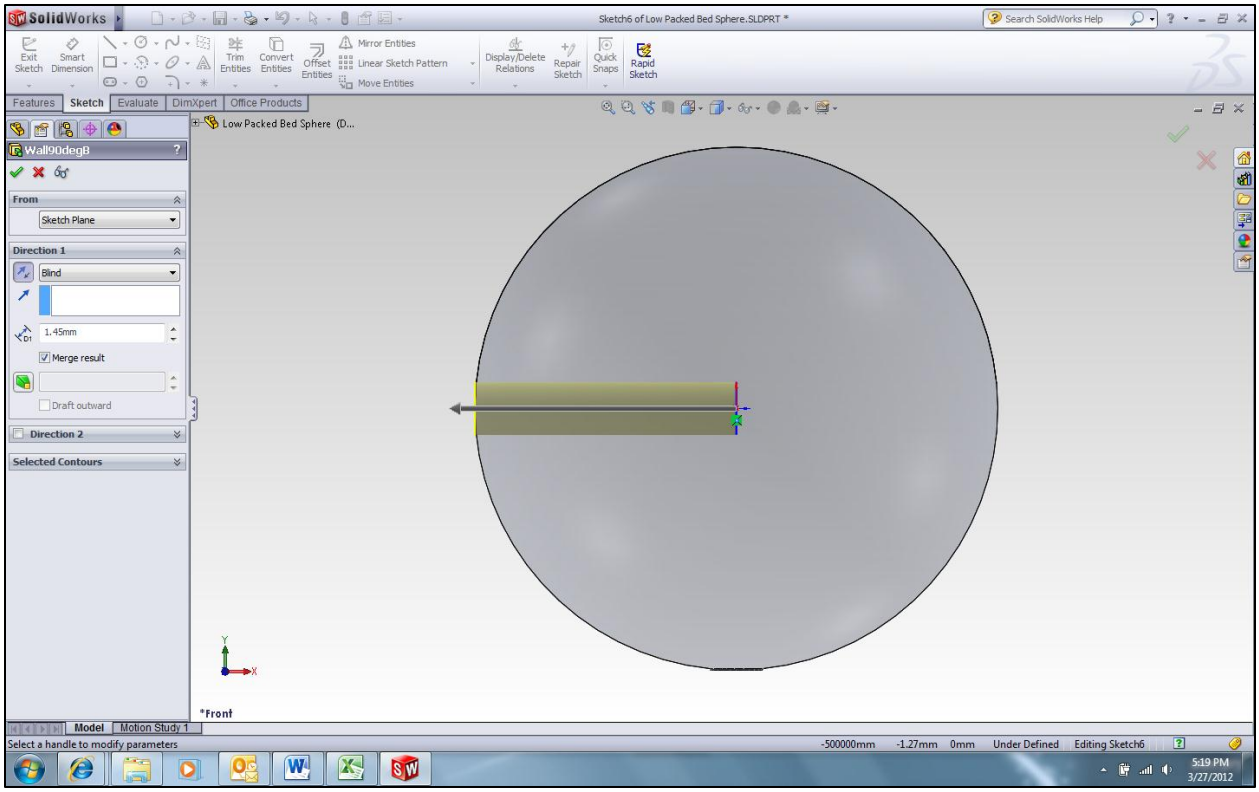

Figure A.2.3: Bridge to the Wall

The contact points between particles were located at the intersection of a plane 0.55mm above the zx-axis, a plane parallel to the yz-plane of a distance of 0.55mm in the negative x-direction and the surface of the sphere. Axes were created from the origin to these contact points. Planes were created perpendicular to the contact points at the origin and the bridges were created.

Bottom-Packed-Model Sphere:

The bridge to the bottom of the channel was drawn on the zx-plane and the bridge to the wall was drawn on the yz-plane. Planes for bridges at the contact points between particles were created by locating where the contact points were, drawing an axis from the contact point to the sphere origin and creating a plane perpendicular to the axis and was also coincident with the origin of the sphere. The contact points between particles were located on the edge of the sphere along the axis formed between the zx-plane and a plane parallel to the yz-plane of a distance of 0.55mm as shown below in [figure xx].

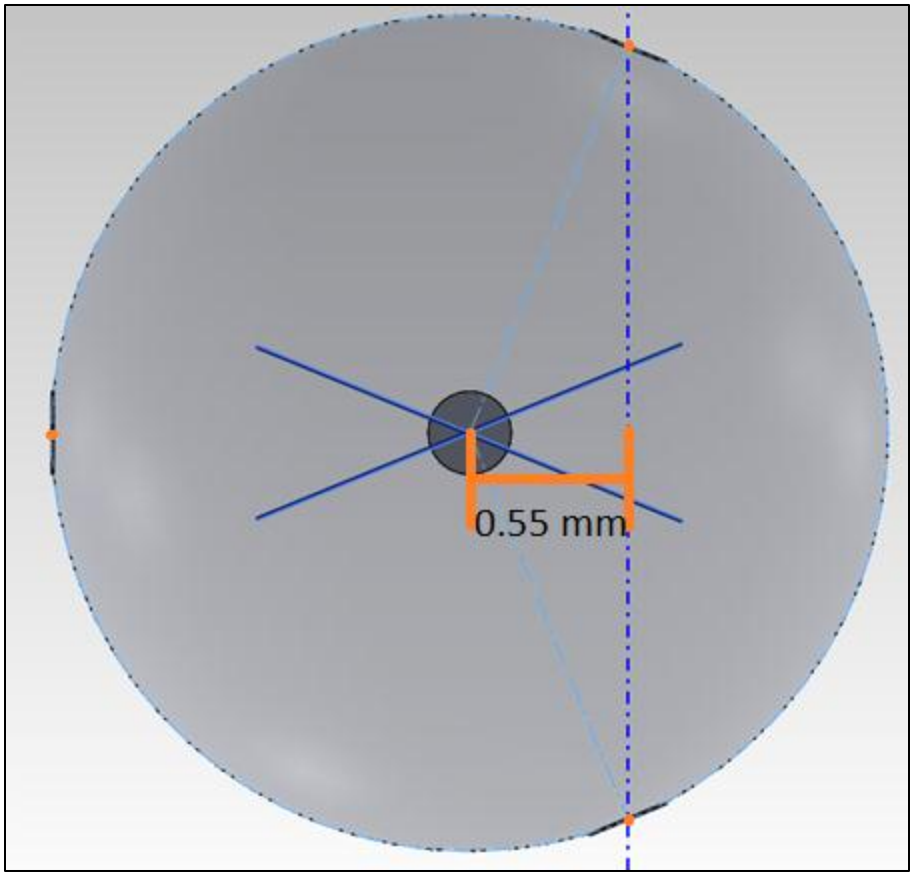

Figure A.2.4: Planes Created for Bottom Sphere Contact Points (zx-axis)

Spiral-Packed-Model Sphere:

The spiral-packed geometry was created similarly to the bottom-packed contact point geometry. The bridge to the bottom of the channel was drawn on the zx-plane and extruded in the negative z direction. The bridge to the wall was drawn on the yz-plane and extruded in the positive x direction. One contact point between particles was located at the intersection between the zx-plane, a plane parallel to the yz-plane at a distance of 0.55mm and the surface of the sphere. Another contact point was located between the zy-plane, a plane parallel to the zx-plane at a distance of 0.55mm and the surface of the sphere. This geometry can be seen below:

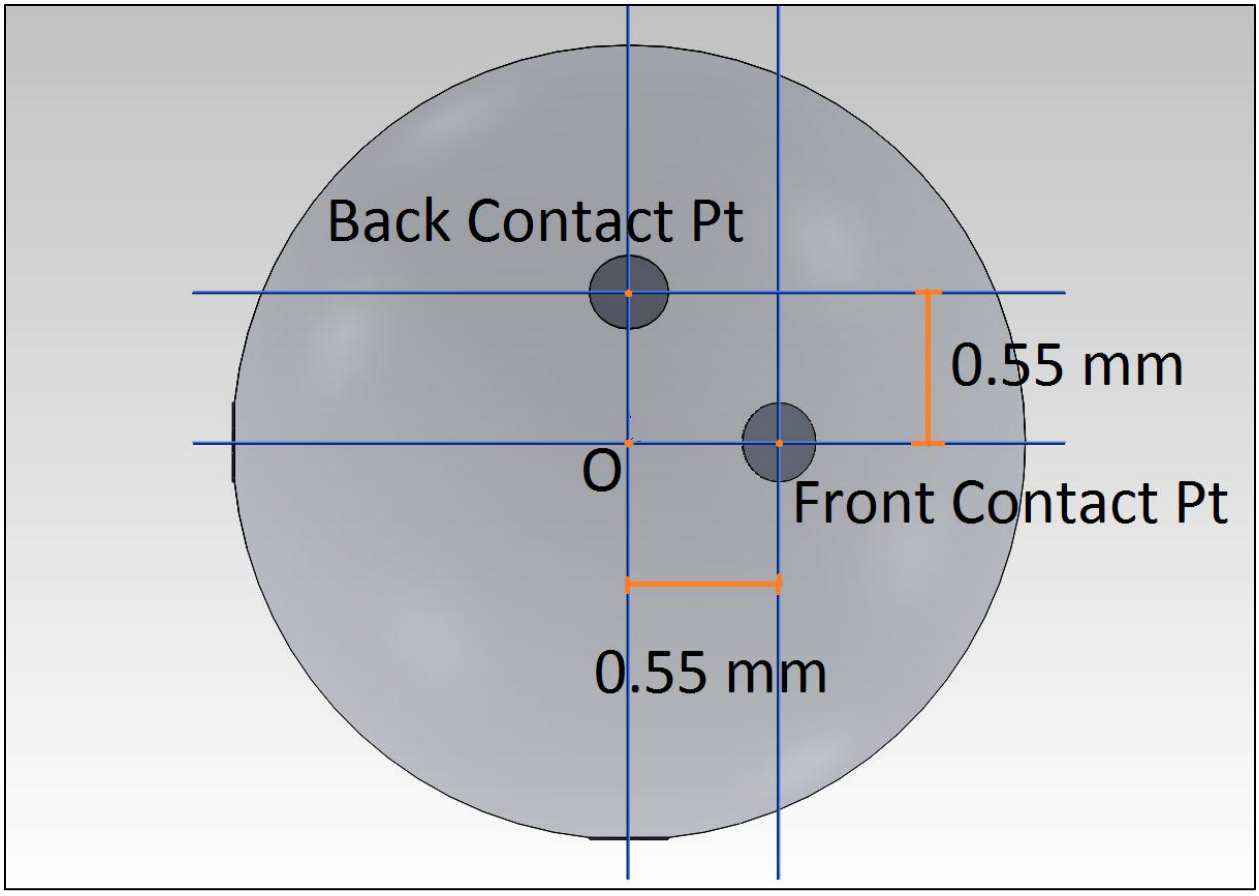

Figure A.2.5: Spiral-Packed Sphere Bridge Geometry (xy-plane)

Appendix B: Sample Calculation for Void Fraction in Diagonally-Packed 1 meter Channel with 408 Spherical Particles

Void fraction equation

$$\varepsilon = \frac{V_{tube} - V_{spheres}}{V_{tube}}$$

Known Variables

$V_{channel}$ = volume of 1m empty channel = 16000 mm^3

V_{sphere} = volume of single particle with 4 bridges = 12.771 mm^3 (from SolidWorks)

Find total volume of spheres, $V_{spheres}$

$$V_{spheres} = 408 V_{sphere}$$

$$V_{spheres} = 408 * 12.771\ mm^3$$

$$V_{spheres} = 5210.589\ mm^3$$

Find void fraction, ε

$$\varepsilon = \frac{16000 mm^3 - 5210.589 mm^3}{16000 mm^3}$$

$$\varepsilon = 0.67$$

Appendix C: Sample Calculation for Single-Phase (liquid water) Pressure Drop in an Empty Channel

Darcy-Weisbach Equation

$$\Delta P = f * \frac{L}{D} * \frac{\rho V^2}{2}$$

Known Variables

L = channel length = 1 m
ρ = fluid (water) density = 998.2 kg/m^3
V = fluid velocity = 0.5 m/s
μ = fluid viscosity = 0.001002 kg/m*s
A = channel cross sectional area = 0.000016 m^2
P = wetted perimeter = 0.016 m

Unknown Variables

D = hydraulic diameter
f = Moody friction factor
*Solve explicitly for D, need to use Re to find f

Find Hydraulic Diameter, D

$$D = \frac{4A}{P}$$

$$D = \frac{4 * 0.000016\, m^2}{0.016\, m}$$

$$D = 0.004\, m$$

Find Reynolds Number, Re

$$Re = \frac{\rho V D}{\mu}$$

$$Re = \frac{\left(998.2\ \frac{kg}{m^3}\right)\left(0.5\,\frac{m}{s}\right)(0.004\, m)}{0.001002\ \frac{kg}{m*s}}$$

$$Re = 1992.415$$

Find Moody Friction Factor, f

$$f = \frac{56.91}{Re}$$

$$f = \frac{56.91}{1992.415}$$

$$f = 0.0240$$

Find Pressure Drop, ΔP

$$\Delta P = (0.0240)\left(\frac{1m}{0.004m}\right)\left(\frac{998.2\frac{kg}{m^3} * \left(0.5\frac{m}{s}\right)^2}{2}\right)$$

$$\Delta P = 891\ Pa$$

Appendix D: Sample Calculation for Multiphase (liquid water and gaseous nitrogen) Pressure Drop in an Empty Channel

Lockhart-Martinelli Method

1) Calculate pressure gradient for each phase individually
    a. Calculate cross sectional area of channel
    b. Calculate mass flux
    c. Calculate Reynolds number
    d. Calculate Haaland friction factor
    e. Calculate pressure gradient
    f. Repeat for second phase
2) Calculate the Lockhart-Martinelli parameter
3) Calculate total multiphase pressure gradient using Crisholm correlation
    a. Calculate pressure gradient multipliers using Crisholm equations
    b. Calculate pressure gradient for each phase using applicable multipliers
    c. Verify that pressure gradients are equal

Pressure Drop for Water

Known Variables

e/D = pipe roughness for glass = 0.000002m
D_H = hydraulic pipe diameter = 0.004m
P_{H2O} = density of water (liq.) = 998.2 kg/m^3
μ_{H2O} = dynamic viscosity of water (liq.) = 0.001002 Pa*s
$\dot{m}_{H2O}$ = mass flowrate of water (liq.) = 0.008 kg/s

Find cross-sectional area, A_c

$$A_c = (D_H)^2$$

$$A_c = (0.004m)^2$$

$$A_c = 0.000016\ m^2$$

Find mass flux, j_{H2O}

$$j = \frac{\dot{m}}{A_c}$$

$$j = \frac{0.008 \frac{kg}{s}}{0.000016\ m^2}$$

$$j = 500 \frac{kg}{m^2 s}$$

Find Reynolds number, Re_{H2O}

$$Re_{H2O} = \frac{j * D_H}{\mu}$$

$$Re_{H2O} = \frac{500 \frac{kg}{m^2 s} * 0.004m}{0.001002\ Pa * s}$$

$$Re_{H2O} = 1996.008$$

Find friction factor, f_{H2O}

$$f_{H2O}^{-0.5} = -1.8log_{10}\left(\left(\frac{\frac{e}{D}}{3.7D_H}\right)^{1.11} + \left(\frac{6.9}{Re_{H2O}}\right)\right)$$

$$f_{H2O}^{-0.5} = -1.8log_{10}\left(\left(\frac{0.000002}{3.7 * 0.004m}\right)^{1.11} + \left(\frac{6.9}{1996.008}\right)\right)$$

$$f_{H2O} = 0.0512$$

Find pressure gradient, $(\Delta P/L)_{H2O}$

$$\left(\frac{\Delta P}{L}\right)_{H2O} = \frac{f_{H2O} * (j_{H2O})^2}{2 * \rho_{H2O} * D_H}$$

$$\left(\frac{\Delta P}{L}\right)_{H2O} = \frac{0.0512 * \left(500 \frac{kg}{m^2 s}\right)^2}{2 * 998.2 \frac{kg}{m^3} * 0.004m}$$

$$\left(\frac{\Delta P}{L}\right)_{H2O} = 1603.204 \frac{Pa}{m}$$

<u>Pressure Drop for Nitrogen</u>

Known Variables

e/D = pipe roughness for glass = 0.000002m
D_H = hydraulic pipe diameter = 0.004m
P_{H2O} = density of nitrogen (gas) = 1.165 kg/m^3
μ_{H2O} = dynamic viscosity of nitrogen (gas) = 0.00001747 Pa*s
$\dot{m}_{H2O}$ = mass flowrate of nitrogen (gas) = 0.0002 kg/s

Find cross-sectional area, A_c

$$A_c = (D_H)^2$$

$$A_c = (0.004m)^2$$

$$A_c = 0.000016\, m^2$$

Find mass flux, j_{N2}

$$j = \frac{\dot{m}}{A_c}$$

$$j = \frac{0.0002 \frac{kg}{s}}{0.000016\, m^2}$$

$$j = 12.5 \frac{kg}{m^2 s}$$

Find Reynolds number, Re_{N2}

$$Re_{N2} = \frac{j * D_H}{\mu}$$

$$Re_{N2} = \frac{12.5 \frac{kg}{m^2 s} * 0.004m}{0.00001747\ Pa * s}$$

$$Re_{N2} = 2862.049$$

Find friction factor, f_{N2}

$$f_{N2}^{-0.5} = -1.8 log_{10}\left(\left(\frac{\frac{e}{D}}{3.7 D_H}\right)^{1.11} + \left(\frac{6.9}{Re_{H2O}}\right)\right)$$

$$f_{N2}^{-0.5} = -1.8 log_{10}\left(\left(\frac{0.000002}{3.7 * 0.004m}\right)^{1.11} + \left(\frac{6.9}{2862.049}\right)\right)$$

$$f_{N2} = 0.0454$$

Find pressure gradient, $(\Delta P/L)_{N2}$

$$\left(\frac{\Delta P}{L}\right)_{N2} = \frac{f_{N2} * (j_{N2})^2}{2 * \rho_{N2} * D_H}$$

$$\left(\frac{\Delta P}{L}\right)_{N2} = \frac{0.0454 * \left(12.5 \frac{kg}{m^2 s}\right)^2}{2 * 1.165 \frac{kg}{m^3} * 0.004m}$$

$$\left(\frac{\Delta P}{L}\right)_{N2} = 760.295 \frac{Pa}{m}$$

Calculate Lockhart-Martinelli Parameter

Find Lockhart-Martinelli parameter, X

$$X = \sqrt{\frac{\left(\frac{\Delta P}{L}\right)_{H_2O}}{\left(\frac{\Delta P}{L}\right)_{N_2}}}$$

$$X = \sqrt{\frac{1603.204 \frac{Pa}{m}}{760.295 \frac{Pa}{m}}}$$

$$X = 1.452$$

Calculate Total Multiphase Pressure Gradient

Find water pressure gradient multiplier (Crisholm Equation), ϕ_{H2O}

$$\phi_{H2O} = (1 + 18x^{-1} + x^{-2})^{0.5}$$

$$\phi_{H2O} = (1 + 18 * (1.452)^{-1} + (1.452)^{-2})^{0.5}$$

$$\phi_{H2O} = 3.724$$

Find nitrogen pressure gradient multiplier (Crisholm Equation), ϕ_{N2}

$$\phi_{N2} = (1 + 18x + x)^{0.5}$$

$$\phi_{N2} = (1 + 18 * 1.452 + (1.452)^2)^{0.5}$$

$$\phi_{N2} = 5.408$$

Find multiphase pressure gradient, $(\Delta P/L)_{multi}$

$$\left(\frac{\Delta P}{L}\right)_{multi} = (\phi_{H2O})^2 \left(\frac{\Delta P}{L}\right)_{H2O} = (\phi_{N2})^2 \left(\frac{\Delta P}{L}\right)_{N2}$$

$$\left(\frac{\Delta P}{L}\right)_{multi} = (3.724)^2\left(1603.204\frac{Pa}{m}\right) = (5.408)^2\left(760.295\frac{Pa}{m}\right)$$

$$\left(\frac{\Delta P}{L}\right)_{multi} = 22236.245\frac{Pa}{m} = 22236.2446\frac{Pa}{m}$$

Appendix E: Sample Calculation for Single-Phase (air) Pressure Drop in a Packed Channel

Ergun Equation

$$\frac{\Delta P}{L} = \frac{150 V_{air} \mu_{air}}{\Phi_s^2 D_p^2} * \frac{(1-\varepsilon)^2}{\varepsilon^3} + \frac{1.75 \rho_{air} V_{air}^2}{\Phi_s D_p} * \frac{1-\varepsilon}{\varepsilon^3}$$

Known Variables

V_{air} = air velocity = 0.5 m/s
μ_{air} = air dynamic viscosity = 0.000018 kg/m*s
ρ_{air} = air density = 1.2041 kg/m^3
Φ_s = particle sphericity = 1
ε = void fraction = 0.67
D_p = particle diameter = 0.0029 m

Find pressure gradient, ΔP/L

$$\frac{\Delta P}{L} = \frac{150 * 0.5 \frac{m}{s} * 0.000018 \frac{kg}{m*s}}{(1)^2 (0.0029m)^2} * \frac{(1-0.67)^2}{(0.67)^3} + \frac{\left(1.75 * 1.2041 \frac{kg}{m^3} * \left(0.5 \frac{m}{s}\right)^2\right)}{1 * 0.0027m} * \frac{1-0.67}{(0.67)^3}$$

$$\frac{\Delta P}{L} = 248.438 \frac{Pa}{m}$$

Appendix F: ANSYS FLUENT Solution Methods for Single and Multiphase Problems

Variables used as inputs for FLUENT Single Phase Trials:

Problem Setup

General

- Pressure Based Solver
- Velocity formulation : Absolute
- Time : Steady State
- Gravity Effects
    - y=-9.8 m/s^2
- Set units :set all to SI

Models

- Multiphase : Off
- Energy :Off
- Viscous : Laminar
- Radiation : Off
- Heat exchangers :Off
- Species :Off
- Discrete phase :Off
- Acoustics :Off

Materials

- Fluid : Water (liquid)
- Solid : Aluminum is default

Cell Zone Conditions

- No specifications made in this section

Boundary Conditions

- Periodic Conditions
    - Specify Water flow rates

Dynamic Mesh

- Not Used

Reference values

- No specifications made in this section, not necessary for calculations to be made

Solution

Solution Methods

- Scheme: Simple
- Spatial Discretization: least squares cell based
- Pressure: Standard
- Momentum: first order upwind

Solution Controls

- Under relaxation factors
  - Pressure: .3
  - Density: 0.5
  - Body Forces: 0.5
  - Momentum: .5

Monitors

- Residuals, statistic and force monitors
  - Residuals: print, plot
    - Continuity- $1*10^{-10}$
  - Statistic: off
  - Drag: off
  - Lift: off
  - Moment: off
- Surf-mon-1
  - Print, Plot
  - Area weighted average inlet total pressure

Solution Initialization

- Initialization methods: Standard
- Reference frame: Absolute
- Initial values
  - Keep all at 0
- Calculation activities
  - Autosave every 0 iterations
- Run calculation
  - Number of iterations:
  - Reporting Interval: 1
  - Profile Update Interval: 1

<u>Variables used as inputs for FLUENT Multiphase Trials:</u>

Problem Setup

General

- Pressure Based Solver
- Velocity formulation : Absolute
- Time : Steady State
- gravity effects
  - $y=-9.8\ m/s^2$
- Set units :set all to SI

Models

- Multiphase : On
  - Eulerian –implicit, 2 Eulerian phases specified
- Energy :Off

- Viscous : Laminar
- Radiation : Off
- Heat exchangers :Off
- Species :Off
- Discrete phase :Off
- Acoustics :Off

Materials
- Fluid : Water (liquid) and Nitrogen (gas)
- Solid : Aluminum is default

Phases
- Primary phase: Nitrogen
- Secondary phase: Water
- Phase interaction: Schiller-Naumann drag coefficient model

Cell Zone Conditions
- No specifications made in this section

Boundary Conditions
    - Periodic Conditions
        - Specify Nitrogen and Water flow rates

Dynamic Mesh
- Not Used

Reference values
- No specifications made in this section, not necessary for calculations to be made

Solution
Solution Methods
- Scheme: multiphase coupled
- Spatial Discretization: least squares cell based
- Momentum: first order upwind
- Volume Fraction: first order upwind

Solution Controls
- Courant Number: 200
- Explicit Relaxation Factor
    - Momentum: 0.5
    - Pressure: 0.3
- Under relaxation factors
    - Density: 0.8
    - Body Forces: 0.8
    - Volume Fraction: 0.5

Monitors

- Residuals, statistic and force monitors
    - Residuals: print, plot
        - Continuity- $1*10^{-10}$
    - Statistic: off
    - Drag: off
    - Lift: off
    - Moment: off
- Surf-mon-1
    - Print, Plot
    - Area weighted average inlet total pressure

Solution Initialization

- Initialization methods: Standard
- Reference frame: Absolute
- Initial values
    - Keep all at 0
- Calculation activities
    - Autosave every (time steps): 100
- Run calculation
    - Time stepping method: Fixed
    - Time step size (s): 1
    - Number of time steps: 1
    - Max iterations/time step: 150
    - Reporting interval: 1
    - Profile update interval: 1